I hereby certify that to the best of my knowledge the material contained in this thesis represents the author's original work. Further it has not been previously submitted for any degree in any institution.

E. St. A. Jordine.

THEORY AND APPLICATIONS OF ELECTROSTATIC MODELS TO THE COLLOIDAL BEHAVIOUR OF CHARGED MACROMOLECULES

by

E. St.A. JORDINE, M.Sc. (University of California, Berkeley)

Submitted in satisfaction of the requirements of the degree of Doctor of Philosophy in the Faculty of Science (Department of Physical and Inorganic Chemistry) University of Adelaide, Adelaide, South Australia.

1964

THEORY AND

ERRATUM: APPLICATION OF ELECTROSTATIC MODELS TO THE COLLOIDAL BEHAVIOUR OF CHARGED MACROMOLECULES.

(Ph.D. Thesis, University of Adelaide)

E. St.A. Jordine.

Submitted 1964.

There are no pages 51-56 and no equations 3-13, 15 and 16.

CONTENTS

F I G U R E S

LEGENDS

TABLES

ACKNOWLEDGEMENTS

I am indebted to Professor C. A. Hurst of the University of Adelaide for enormous mathematical assistance.

I wish to thank Mr. R. B. Lewis, Master of St. Mark's College(University of Adelaide) and Professor D. O. Jordan of the University of Adelaide for availing me of the facilities of their establishments.

SUMMARY

In this work an effort has been made to develop a theory capable of explaining some of the stability relations of charged colloidal macromolecules and lamellar crystals quantitative manner, using potential energy curves. Emphasis is on regions of close approach between particles where there is no Boltzmann distribution of ions and where the systems are essentially heterogenous crystals behave essentially like solids. We can safely treat the problem as one of solid state physics. In this region, that is at particle-particle separations $2D<30\text{Å}$, all the known theories based on fluids have failed. It also happens that phenomena such as coagulation occur in this region since this is where the main energy barriers occur.

While the entire theory is based on electrostatics, as is double-layer theory for example, it differs radically in approach from all the other works to date except in some respects for Langmuir's (22). Some of

these differences are: the van der Waals-London forces which are really weak electrical forces are completely ignored; Boltzmann's theorem is not assumed; nor is a volume density of charge necessarily prescribed. On the other hand some new concepts have been introduced, such as the importance of repulsive image forces, solvent ion interaction and the importance of the dielectric properties of all the systems involved.

In the first chapter the problems of the field of colloid science and the need for a radically new approach are presented. Chapter II outlines the philosophy behind the theory, suggesting the approach be biased by the physical situation rather than by mathematical expedients.

Chapter III states the problem for plate-shaped particles (special reference to montmorillonite) and suggests a solid state to solid-liquid approach, rather than the usual approach biased towards fluids. This is followed by the derivation of suitable potential functions using the image and Fourier methods in Chapter IV, and the final evaluation of the electrostatic energy of interaction in Chapter V. In Chapter IV some consequences of the image method are shown to involve concepts of the theory of sets. The equivalence of the image and Fourier methods is shown and extensions made to consider membranes and monolayers and two dimensional ionic crystal lattices.

In Chapter VI an outline of the mechanism of ion-solvent, plate-shaped particle interaction is given and an empirical relation for the specific ion-solvent energy of interaction is obtained. The question of dielectric saturation is discussed briefly.

In Chapter VII we return to the energy equations of Chapter V and compute the potential energy curves. We then develop a special bounded nonlinear surface charge potential function and thus improve the linear ones of Chapter IV. These functions are tested by comparison with experiment, found adequate, and therefore offered as a contribution to classical physics.

A so-called J-factor is introduced which serves the purpose of a damping factor for the nonlinear potential function. It is shown to be related to factors such as electrolyte concentration and the area and charge density of the macromolecule. Since J is at the moment an empirical parameter it has yet to be justified theoretically.

It must be stressed that the nonlinear potential functions introduced in Chapter VII are only empirical at the moment and hence would not satisfy the linear differential equations of Chapter IV. It is up to the theoretical physicists to reconcile this situation.

For the benefit of the reader the image and Fourier developments are self contained hence either method in Chapters IV and V may be followed through separately.

In Chapter VIII the general discussion and concluding remarks are presented. Briefly this may be stated as follows: the role of the hydration energy or solvent-ion interaction on the stability relations between two plate-shaped particles (montmorillonite, vermiculite) is that of a trigger mechanism for what seems to be basically an electrostatic process. The general behaviour of the potential energy is shown to be such a function of distance as to demonstrate a repulsive force for small separations leading into an energy well or minimum for intermediate separations. This is followed by maximum and thereafter a path of decreasing energy, which gradually vanes, due to edge effects becoming important at large separations. The foregoing is shown to be in complete accord with accumulated experimental findings over the years. Physically, the basis of the shape of the energy curve is that at small separations the repulsive ion-solvent and ion-image forces prevail whereas at intermediate distances the attractive surface-ion terms become important; finally the surface-surface and ion-image terms dominate at larger distances.

This type of behaviour is shown in chapter VIII to explain many surface phenomena, such as stability of living tissues, perhaps nerve impulses, consolidation behaviour of clay soils and certain features of thixotropy.

It is concluded without reservations that for particle-particle separations of large plate-shaped particles which lie below 30Å the theory is adequate if not excellent. This is precisely the region where previous theories have failed. Moreover it is a most important region for coagulation phenomena.

In the final section of chapter VIII an outline is given on the treatment of the interaction between spherical particles in a bipolar coacervate.

Though this work is not concerned with double-layer theory, we cannot ignore it since it is so well known. In chapter I we outlined its many pitfalls and errors in selecting boundary conditions. At this point the author must stress that double-layer theory is based completely on electrostatics with a volume density of charge defined by Boltzmann's theorem. In as much as the Boltzmann's distribution function is of the form $e^{-u/kT}$ it is clear that if the reaction occurs

isothermally, as in most colloid systemskT is just a constant. In other words kT does not depend on coordinates and hence the form of the potential energy (for a given model) is quite independent of kT. Even in the energy equations obtained in (33), kT is only a scale factor.

Moreover, if U, the binding energy, is much greater than kT, then we see at once that $e^{-U/kT}$ ~ zero.

Since however the so-called double-layer theory has been used for so many years as the standard treatment for colloid systems over all particle-particle separations, an endeavour is made in the appendix to put it in proper perspective. It is shown that the image forces which have been ignored in (33) can be incorporated. Further the free surface charge on the macromolecule should not be ignored completely. We outline a solution as in(33) assuming Boltzmann's theorem for the volume density of charge so selected as to satisfy all the boundary conditions of Chapter IV. Finally we show that this approach and that of prescribed electrostatic models, are not mutually exclusive but are complementary just as the equilibrium and orbit theories of plasma physics are complementary.

Thus as a final plea let us restrict double-layer theory to separations, $2D > 30\text{Å}$.

PART I

C H A P T E R I

INTRODUCTION

1. Colloidal Phenomena

Few areas of science can claim such a diverse impact on the various disciplines or even on everyday existence; from the paint maker's pot to the housewife's pudding. It is not the purpose of this work to display concern with the semantics which could be generated by formally considering the limits and definition of a colloidal system. Such topics are properly the province of the pedant. It will become apparent however from the systems and phenomena selected for discussion and possible elucidation just what is the frame of reference for the subheading above.

The area of colloid science, perhaps occupies an intermediate position both with respect to state of matter and dimensions. In the first instance it may be considered in a formal sense to occupy a borderline state in the regions of solid-gas, liquid-liquid, liquid-gas, liquid-solid and solid states. In this work we will be concerned with liquid-solid to solid systems. From the point of view of dimensions of systems of interest, it is intermediate

to the classical interests of physicists and chemists on one hand and that of the structure, ceramic and civil engineers on the other. It spans the inanimate to the living, and is intimately bound up with plant and animal tissue by virtue of its relation to surface phenomena, membranes and gel structure.

Thus it claims the attention of the biologist, the engineer, the agriculturist, the chemist and the physicist.

What are some of these phenomena which are related to various macroscopic behaviours of systems? ... stability of suspensions, gelation of systems, thixotropy, rheopexy and coagulation. These influence such processes as the ability of plant roots to penetrate the soil and respire, the strength of foundations and buildings, quick clays, tendency of paints to settle when left to stand or run when brushed, tendency of dams to creak, molding of ceramic structures or even the ability of the human body to subsist and function.

There is little doubt that for a system to progress from a dispersed state to a coagulated state, or from a dry powder to a thixotropic gel, there must be driving forces positive and negative in sign and regions of null or equilibrium.

It is the physical principles underlying some of these phenomena, that it is proposed to investigate. Clearly this is a formidable task within the limits of available time and effort, nonetheless a useful if not representative selection can be made. Chief among those selected for investigation will be the general question of the stability of mutually interacting colloidal particles.

2. Problems of the Field

It is fair to say, that this area of endeavour, has subsisted over the years as essentially an art. By and large, the complexity and multiplicity of interacting constituents have defied substantial analysis. As in all fields however where time and abundance allows, it is usually possible by laborious trial and error to build up a body of empirical if not pragmatic knowledge, sufficient for day to day existence. Thus every day engineering processes even if restricted to safe tolerances, are not prevented by such lack of analysis.

Among the major problems is the question of geometries of ponderable constituents. An essential way to at least initial progress in any field, is the making of simplifying assumptions and the study of the associated simple systems. Since there is the

possibility of approximating systems to a manageable range of geometries, some of these problems can be partially surmounted. The possibility exists for example of approximating some colloidal particles to discs cylinders or even spheres.

Other problems such as distribution functions for constituents of atomic dimensions, also have a bearing on geometry. To select a distribution function, substantial experimental evidence on a micro-level or a correct guiding hypothesis is required. For example we may desire to know, what would be the distribution of counter ions in the intervening solvent medium between two charged plate-shaped macromolecules separated by a distance, 2D. To such questions there is no simple answer.

3. Current Theories

Perhaps the most current is that expounded in Verwey and Overbeek's book "Theory of Stability of Lyophobic Colloids" (33). This book has been the standard work for many years and as a result it has been very much over used if not misused. The very first works on this double-layer concept are due to Gouy (14, 15) and Chapman (8) with contributions from Debye and

Huckel (9) and modifications by Stern (31). In general, these workers were more interested in electrochemistry rather than colloid stability. In the appendix of (33) a critical survey of the work on colloid stability since 1925 to the date of writing (1948) is given. This is well worth reading since Langmuir's work (22) which will be discussed in section 5 of this chapter is singled out as being iconoclastic and most severely criticised.

Essentially the theory* in (33) is based on electrostatics, and relies exclusively on the equilibrium assumption in defining the volume density of charge in Poisson's equation. In other words the distribution of counter ions and excess electrolyte is assumed to be defined by Boltzmann's theorem. This is essentially the same general approach as Debye and Huckel (9) used in considering electrolytes.

The treatment in (33) shows that a solution to Poisson's equation leads always to a repulsive force between two interacting double layers. It becomes necessary therefore in (33) to have recourse to the so-called

---

* Stern (31). (33) however modifies this by assuming a condenser type distribution of counter ions in the immediate neighbourhood of the macromolecular surface. The author prefers this approach in principle.

attractive van der Waals-London forces, in order to counter-balance the repulsion and facilitate coagulation and stability. These phenomena are related to points of the potential energy curves corresponding to extrema or null points of force.

Nearly all the work in (33) relates to the case of two infinite planes, with only a limited treatment for spherical particles. Not that in this work, it will be possible to proceed to other geometries.

4. Pitfalls and Failures of Current Theories

These may be regarded to be of two types, the first based on physical considerations and the second based on mathematical considerations. The ultimate test is necessarily the first, since while elegant but hasty mathematical generalisations might elicit skilful mathematical analysis, it will never really further our understanding of science.

In all these theories concerning plate-shaped particles, the assumption is usually made that the particles are infinitely thick conductors. No effort is made to consider the dielectric properties of the macromolecules or the influence of its finite thickness. The free surface charge on the particles is not explicitly

taken into account, although for most systems the surface bears some free charge. Other important phenomena such as the dielectric saturation of the solvent medium and important specific counter ion effects, such as coordination of solvent molecules, are not considered seriously even though they must have immense influence on peptization and other phenomena.

There is also the philosophic question basic to these theories. Can a true equilibrium density be defined over any extensive region of space for a static condensed system* ... rather than a hydro-kinetic effect.

This last point leads into one of the main mathematical questions. The fact that the distribution function for the density is such a function of the electrostatic potential, as to lead to a non-linear differential equation, conflicts with the linear superposition theorem of classical electrostatics. Nonetheless this point is minor in comparison with such physical atrocities as regarding the macromolecule as an infinitely thick conductor. This last assumption is equivalent to assigning a value of infinity to the dielectric constant of the macromolecule.

In view of all this it is impressed upon the author that physics may have been sacrificed at the expense

* Of thermal equilibrium throughout a condensed system is $\frac{1}{V}\int \rho dv'$ different from zero?

of obtaining an approximate solution in closed form, to a differential equation.

Finally there is the question of the exact role of the van der Waals-London forces, which are in reality a manifestation of weak electrical forces. Further discussion on this will be pursued in section 5 which deals with Langmuir's work (22). It may be remarked however, that the van der Waals-London energy for plate-shaped particles, produces binding energies which are not even comparable to the ordinary thermal energy of the particles (27).

Sufficient has been said to indicate that there are very serious and disturbing features about the current theories.

5. Langmuir's Work (22): Role of van der Waals-London Forces

Langmuir was the first to insist that many aspects of colloid stability must have their basis in coulomb forces. He urged quite strongly, that the exact role of the van der Waals-London forces which are supposed to act at a distance independent of the intervening solvent medium in the colloidal system, was suspect if not spurious.

Langmuir (22) considered the colloid system as being similar to a saturated solution of an ionic crystalline salt. Thus the process of unipolar coacervation for example, is regarded as being analogous to the formation of a crystal from a saturated salt solution. The counter ions of the macromolecules must therefore have reasonable specific energies of interaction, as opposed to a general field effect which would be the situation if there were a prescribed volume density of charge. Despite all this his treatment is sketchy in parts and is also based on a definable volume density of charge. In addition he considered the colloidal system as a whole, in keeping with the analogy to the saturated salt solution consisting of equal amounts of positive and negative charges on the ions. Langmuir (22) points out that in a similar way to the formation of the ionic crystal, there is the tendency for the colloid system as a whole, to contract under the influence of attractive coulomb forces between counter ions and macromolecules. He further points out that in order to counter balance this tendency to contract, some repulsive force, possibly hydration of the ions, must be found. This he says would contribute to the formation of mall or equilibrium of forces between the particles and ensure unipolar coacervation. As further evidence he cites the fact,

that not only in unipolar coacervates (colloidal particles in the system having charge of a single sign + or -), but also in bipolar coacervates (particles with charges of opposite sign) the colloidal particles remain separated by considerable distances and do not come into contact.

After duly considering Langmuir's propositions the author is of the opinion that Langmuir has been singled out for severe and unreasonable criticism in (33). Perhaps in the following pages we may show that Langmuir (22) was in fact correct.

6. Need for New Approach and or Modifications

The foregoing demonstrates the many aspects of the problem to be resolved and clarified both physically and mathematically. Foremost among these are the considerations of the dielectric properties of the respective media, their finite width and extent. The usual models of two plane uncharged conducting interfaces, is a most artificial and incomplete model.

It is essential to distinguish between the role played by the equivalent counter ions neutralising the free charge on the macromolecule, as opposed to the excess electrolyte which may be present in the system. This is intimately related to peptization phenomena and

the influence of the amount of charge on the counter ion, (in chemical terms the influence of the valency of the ions) on colloid stability. For instance nearly all known unipolar colloidal systems having polyvalent counter ions remain undispersed when placed in a pure liquid solvent, irrespective of the solvent.

Lastly there is the question again of the validity of the use of Boltzmann's theorem to define a volume density of charge in a condensed system, or even the existence of a macroscopic volume density under any conditions of static equilibrium.

7. Scope of this Work

The main purpose is to evolve more realistic models of known systems and to obtain relations connecting some of the electrostatic phenomena involved. As the title of this work implies, the equilibrium assumption will not be made, and consideration will be given to the points mentioned in the previous sections.

As will be seen, an attempt will be made to approach the problem in a manner satisfactory to physics. Firstly, knowing as much as possible about the physical nature of the system, we select functions of such a general form, that they automatically satisfy the more rigid

mathematical analysis. Later, these functions must also evolve into manipulable functions, which satisfy the boundary conditions at every interface of finite regions and regions extending to infinity. Finally they must have the proper order at infinity.

Most workers over the years have confined their attention to plate-shaped particles. Aside from being representative of commercially important systems such as the BENTONE® gellants, it is the most manageable geometry. In addition there exists an excellent body of experimental information (2,3,4,5,26,27) with which to test a theory. Nonetheless spheres will be considered briefly.

It must be pointed out that depending on relative dimensions, every figure can be approximated to a plane, and since a plane needs no generator, it is basic to all other geometries. We therefore shall regard it as the starting point for any theory to be developed. Thus due to limits of available time and effort we agree to restrict the development to plane geometries almost exclusively.

Several aspects of the development will be seen to be directly applicable to lamellar crystals with

---

® Patent, National Lead Co., U.S.A.

imperfections, and as such represent contributions to solid state physics. On the other hand several questions will arise which demonstrate the incompleteness of classical physics and at the same time furnish interesting physical analogies to aspects of set theories.

As a matter of fact the general problem developed in this work has already in part been concisely set out in two recent communications to the Journal of Chemical Physics and the Bulletin of the Chemical Society, Japan.

CHAPTER II

THEORY OF ELECTROSTATIC MODELS

1. General Features and Mode of Attack

As pointed out in Chapter I the theoretical approach to most colloidal problems, has usually been based on the equilibrium assumption, that is, a Boltzmann distribution of ions is assumed to exist in the neighbourhood of the macromolecular surface in question. It would appear however, that for systems which possess considerable symmetry, the distribution of counter ions in the immediate neighbourhood of the surfaces may be prescribed by symmetry considerations. This leads to the construction of manageable electrostatic models, which are capable of describing the specific interactions of the ions with the surface. The two methods described above, are in a way essentially analagous to the equilibrium and orbit theories of plasma physics and are not necessarily mutually exclusive.

While for ordinary* colloidal systems the use of electrostatic models may not be valid much beyond

---

* For large swelling lamellar crystals such as, [illegible], vermiculite, the model may be used for greater separations as will be explained later.

particle-particle separations, $0 < 2b \leq 30\text{Å}$, it is precisely in this region that the equilibrium approach fails catastrophically. Moreover it is just in this region that some of the most important colloidal phenomena occur.

The idea of specific ion interactions, may be regarded as being inherent in the proposals of Stern (34) and Langmuir (22), especially Stern (34). It was however proposed by the author in (20,21) quite independent of Stern's or Langmuir's work.

The foregoing describes the general features of the theory from the physical point of view largely. In Chapter III justification will be given for these assumptions in regard to plate-shaped macromolecules.

The mathematical features of the theory or the mode of attack will now be considered. Mathematically, the approach is the direct method for boundary value problems. To begin with, every mathematician is aware that it is very rarely ever possible to find a complete solution to a differential equation and that it is always easy to differentiate a function but integration is another problem. With this in mind the aim is always to assume solutions, which without pretence automatically satisfy the differential equations in

question. Now since a reasonable knowledge of the physical situation is usually available, the main criteria thereafter, is to demand that the boundary conditions be satisfied, and that the function has the correct behaviour at infinity.

For electrostatic problems consisting essentially of infinite plane interfaces, the techniques which naturally present themselves, are the image and Fourier transform methods. Ultimately it will be seen that there is no difference between the results of the two methods. They are just different generator mechanisms which accomplish the same end. The Fourier transform method is of course more general, since the potential functions it can represent, need not be continuous everywhere. We may say that the method of electrostatic images is a geometrical generator, while the Fourier transform method is analytic. It will be seen that both methods generate well known Bessel functions.

2. Infinite Sets of Electrostatic Images

The artifice of electrostatic images is well known and owes its origin to Lord Kelvin. According to Maxwell (24) Kelvin's first contributions appeared in Cambridge and Dublin Mathematical Journal (1848) and

Cambridge Mathematical Journal (1853). A fairly complete coverage is to be found in Kelvin's Collected Papers on Electrostatics and Magnetism (32), p. 60-85, p. 86-97 and p. 144-177. Of particular interest are p. 86-97 reprinted from Philosophical Magazine April and August (1853) where he treats the infinite sets of electrostatic images due to two mutually influencing spheres.

We are made to understand in (24, p.281) that this said problem has attracted the attention of many mathematicians, among whom are Poisson, Plana, Cayley, Kirchoff and Mascart. More recently we have Barnes (1) and Russel (28). The last worker (28) has put it to practical use, in the computations of the capacity of spherical electrodes. There is no record of a solution to the corresponding energy problem for the case of infinite sets of images in two or more slabs of dielectric. Although the image method is ideally suited for plane interfaces, it has serious limitations if the regions under study are multiply disconnected. Consider the special case of two slabs of dielectric, located on either side of a point charge. Unless both slabs are infinitely thick, the method of images leads to an everywhere dense point set of images in the regions of interest. As a consequence the functions for the potential will not be analytic. The method seems limited to regions having no more than two plane interfaces.

In other words the regions can be connected by a single slit. There does seem to be some interesting topological questions involved. Affuller discussion will be given later in the development.

3. Fourier Transform Methods

This method is a well known operational technique and is ideally suited to potential porblems of regions having plane interfaces extending to infinity. Since the the functions must form a complete orthonormal system, the useful applications of this method are limited to problems in two dimensions. Such features as multiply disconnected regions and a finite number of discontinuities, do not limit the representation of a function by Fourier transforms.
Hence, for electrostatic models where the image method is unmamageable, this method will be used. Their equivalence for other models will be demonstrated.

PART II

(INTERACTION BETWEEN PLATE-SHAPED PARTICLES OR PLANE SURFACES AND COUNTER IONS - MACROMOLECULES, MONOLAYERS, MEMBRANES)

CHAPTER III

STATEMENT OF PROBLEM AND ELECTROSTATIC MODELS

1. Statement of Problem

The first problem to be considered, is that of the general question of the stability of two or more plate-shaped macromolecules. By this it is meant, the forces governing their tendency to assume definite equilibrium positions with respect to each other in a colloid system. The second problem is much simpler. It relates to the binding of ions and perhaps to the surface pressures on membranes and monolayers. It perhaps may also apply, in a limited way, to the case of ionised monolayers. It will be seen that this is only a limiting case of the first problem. A solution to the first problem will therefore be sought in the first instance, following which, the second problem can thereafter be derived.

Perhaps the best known plate-shaped macromolecules* are those which derive from the clay mineral montmorillonite. The counter ions may be exchanged quite readily to yield homionic forms which exhibit various unusual physical properties. Chief among these, is the tendency of some forms to swell in polar solvents, especially water, to several times their initial volumes, giving thixotropic gels. Such properties are of importance in several branches of engineering, agriculture and industrial chemistry.

The swelling and other colloidal properties of montmorillonite, have been the subject of considerable experimental study over the past thirty years. Typical contributions which may be cited in this regard are Barshad (3), Jordan (19) and Norrish (26).

Perhaps the first systematic theoretical approach, to satisfy the experimental findings with respect to electrostatic parameters, has been due to Jordine, Bodman and Gold (20) and Jordine (21), who applied the method of images in dielectrics. This treatment was a crude beginning of the more comprehensive theory to be developed in this work.

---

* Other plate-shaped macromolecules are colloidal mica, vermiculite and some iron oxide sols.

The studies of montmorillonite with the aid of the electron microscope (20), have shown that the crystals of montmorillonite have lateral dimensions of the order of thousands of angstroms. Maegdefrau (25) and Norrish (26) consider that at close approach of two of the platelets constituting the crystal, the counter ions become ordered between their two immense areas, permitting strong specific interactions. A similar suggestion in even more general terms was made by Langmuir (22), and has already been discussed in Chapter I.

The counter ions may therefore be considered to a first approximation, as having specific areas* of interaction with additive effects; quite analogous to the specific orbits describing the interactions in plasma physics. Derjaguin (12), makes a similar assumption concerning volume elements of polarization, which he justifies for small particle-particle separations. The main requirement for this model to hold, is that the macromolecules should have large surface areas per counter ion and also absolutely. While edge effects are important, montmorillonite or vermiculite platelets with such immense surface areas (20), (13), (27) should be

---

* This point will be considered in more detail at a later stage in the development of the theory, Chapters IV and V.

very suitable systems for treatment in the crystalline and near crystalline regions of swelling. In other words it will not be assumed as most authors of the current theories to date have done, that a Boltzmann distribution of ions is maintained in the neighbourhood of the surface. It is well known that even for fairly ideal systems in the gas phase, the equilibrium assumption has been found wanting.

To a first approximation therefore, the interaction of the counter ions will be considered as being additive, and the platelets as infinite slabs of dielectric. As stated earlier the platelets of montmorillonite are usually organized in groups of perhaps five, ten or more yielding crystals. Now, it is not a simple matter to treat ten platelets at once, but it is possible to treat two, by models which simulate the actual situation. The models which will be selected shall be as general as possible, and are not necessarily restricted to montmorillonite or bentonite (montmorillonite is the main constituent of bentonite).

2. Electrostatic Models

Proceeding on the above assumptions, three

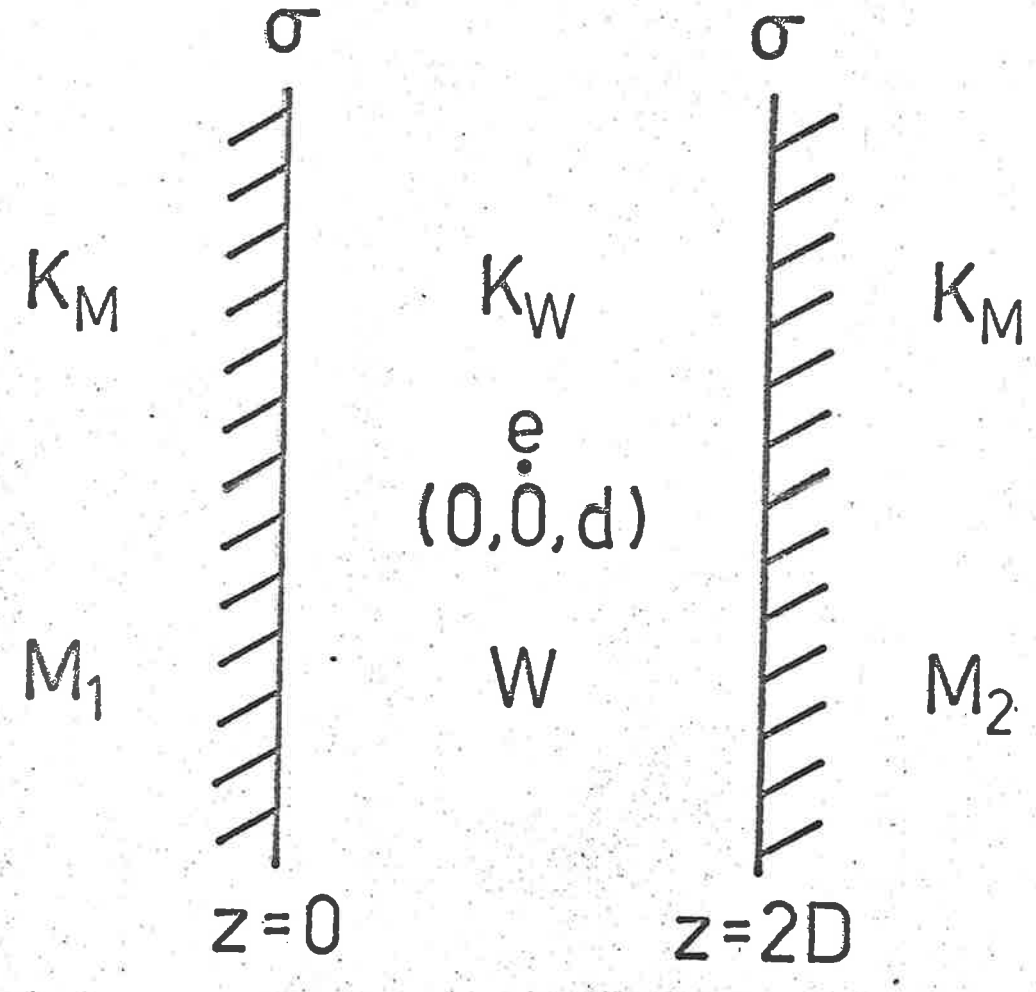

Fig. 1(a) Diagram for Model I

Fig. 1(b) Diagram for Model II

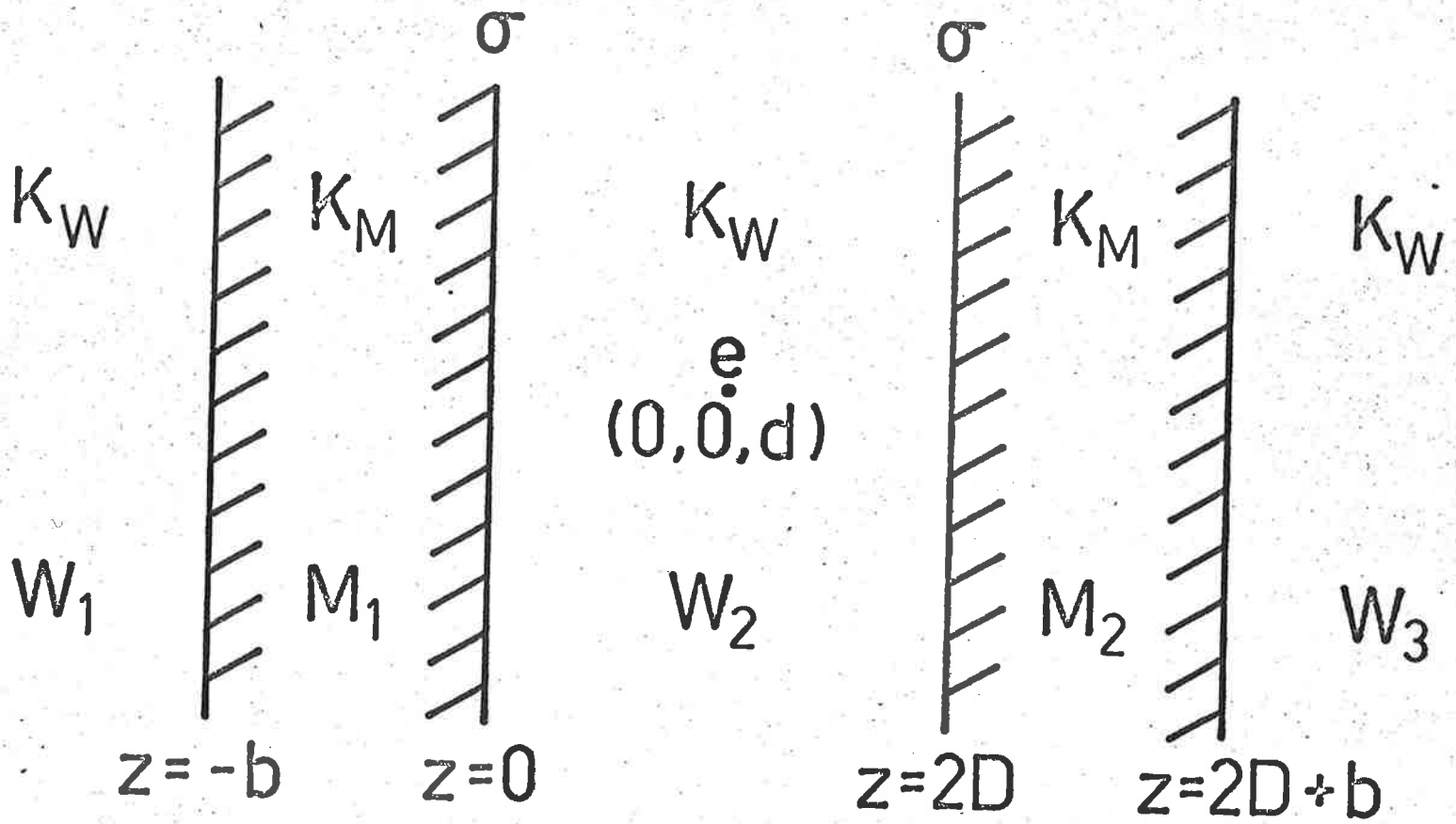

different electrostatic models depicted below as figures 1(a) and 1(b) will be considered. In all the models the plane faces or lateral dimensions of the slabs, are coincident with the planes Z= constant. The models are not all distinct and hence require only two figures. The first model, designated model I, consists of two infinite slabs of dielectric, each of dielectric constant K_M, occupying regions Z< 0 and Z< 2D respectively, with the space 0< Z< 2D filled with a different material (usually water) of dielectric constant K_W. A point charge* e' is situated at the point with coordinates (0,0,d) (0< d< 2D), and the surfaces Z=0 and Z=2D each have a uniform surface charge σ per unit area.

The second model, model II, has two slabs of dielectric material of dielectric constant K_M, occupying the regions -b< Z< 0 and 2D< Z< 2D+b respectively, and the remaining regions are all filled with material of dielectric constant K_W. Once again a point charge is located at (0,0,d), (0< d< 2D) and the surfaces Z=0 and Z=2D are covered with charge σ per unit area. For the

---

* In fact there are usually several such ions evenly spaced in the plane Z=d, but since we have agreed that their effects are additive we may consider one ion at a time. This matter will be discussed further in Chapters IV and V.

surfaces $Z=-b$ and $Z=2D+b$ two possible choices can be made. One is that they are also covered with charge σ per unit area, whilst the other is that they are uncharged. To distinguish these two cases, denote them by model II(a) and model II(b) respectively. Model II(a) thus describes an idealised version (since it violates the principle of electrical neutrality) of two montmorillonite platelets, with the observed surface charge on all faces. Model II(b) is designed to account in a simple way, for the effective neutralization of the outer charges by the presence of other ions, which are not explicitly taken into account. Actually the differences between the two models in the detailed calculations is only minor.

Model II may be extended still further to include the case where K_w in regions W_1 and W_3 differs from W_2. Finally there is the case in which regions W_1 and W_3 have a "volume density of charge." These two extensions will be discussed in Chapter V when considering the energy.

The assignment of a uniform surface charge, σ per unit area, to the surfaces of the slabs in the case of macromolecules derived from the clay minerals, deserves further comment. The negative charge on the surface of the platelets of montmorillonite, arises from isomorphous substitution within the crystal lattice.

Frequently this involves the replacement of Al^{+++} by Mg^{++} in the octahedral layer. It follows therefore from the crystal structure*, that the oxygens in the crystal will have unsatisfied negative charges, which the positive counter ions must satisfy. Now the boundary or immediate periphery of the platelets are composed of oxygen atoms. These are highly electronegative atoms, which will most likely be so polarised, as to accept any excess of negative charge in the interior of the lattice. There are several such oxygens per excess electronic charge, and since there is no physical reason to prefer one atom to the other, the time average at the surface will be representative of the surface charge. Actually the concept of a surface charge or charge cloud as opposed to a pin point charge, is more in harmony with modern physics.

Whatever the actual situation may be, we shall apply this model, with a willingness, to let experiment be the sole arbiter.

---

* See figures 13 and 14 in Appendix 2 for elucidation.

CHAPTER IV

DERIVATION OF POTENTIAL FUNCTIONS

1. General Boundary Conditions

If V_{M_1}, V_{M_2}, V_W denote the potentials in the regions labelled M_1, M_2 and W in figure 1(a) and V_{S_1}, V_{S_2}, V_{W_3}, V_{M_1}, V_{M_2}, the potentials in the corresponding regions shown in figure 1(b), the problem in the case of models I, II(a) and II(b), is to find a solution of the equations

$$\nabla^2 V = 0 \qquad \text{IV - (1)}$$

holding throughout in M_1, M_2, W_1 and W_3, and

$$\nabla^2 V = -\frac{4\pi\sigma}{\kappa_W}\delta(x)\delta(y)\delta(z-a) \qquad \text{IV - (2)}$$

in the regions W and W_2. The symbol $\delta(x)$ denotes the Dirac δ-function, and represents physically a point source at x= 0. In addition to satisfying the equations IV-(1) and -(2) the potential V, must satisfy boundary conditions at the interfaces between regions of different dielectric constants, and also at infinity. We require that the potential V must be continuous at all

interfaces, and that the normal component of the electric displacement be discontinuous according to

$$K_1 \left[\frac{\partial V}{\partial z}\right]_1 - K_2 \left[\frac{\partial V}{\partial z}\right]_2 = -4\pi\sigma_{1,2} \qquad \text{IV - (3)}$$

where $\sigma_{1,2}$ is the charge density on the surface separating regions 1 and 2 with z in region 1 greater than in region 2. The condition at infinity will be discussed later.

No modifications are required for the extension of model II where K_W in regions W_1 and W_3 differs from that in W_2 except for the appropriate changes in K_W. The changes required when there is a volume density of charge in regions W_1 and W_3 are simply that equation IV-(1) must hold in M_1 and M_2 and equation IV-(2) in W_1, W_2 and W_3. For completeness equation IV-(2) may be replaced by

$$\nabla^2 V = \frac{-4\pi}{K_W} \sum_i e_i \, \delta(x-x_i)\delta(y-y_i)\delta(z-z_i) \qquad \text{IV - (4)}$$

The discontinuity in IV-(3) can be removed by separating V into two parts:

$$V = V_1 + V_\sigma \qquad \text{IV - (5)}$$

such that V_1 is the potential due to the ion and its

images and V_σ that due to the surface charges only. Because of the linearity of equations IV-(1) and -(2) V can be taken to satisfy equation IV-(1) everywhere and the boundary condition IV-(3), whilst V_1 satisfies equation IV-(2) in W or W_2 (and equation IV-(1) elsewhere) and satisfies the boundary condition IV-(3) with $\sigma_{,2}$ put equal to zero. With these choices V defined by equation IV-(5) satisfies all requirements.

2. Model I via Image Methods

As a starting point for the model, consider an intense point source of light between two mirrors. If the source is sufficiently bright and the mirrors infinite in extent, an infinite number of images will be generated by successive reflections. By locating the source at (0,0,d), and letting the mirrors be coincident with the surfaces Z=0 and Z=2D, it is easy to show that the Z coordinates of the images will be $Z=4(n+1)D\pm d$, $-[4nD+d]$ and $-[4(n+1)D-d]$ respectively for $n=0,1,2\ldots$ When the source is symmetrically located, that is $\beta = d/2D = \frac{1}{2}$ these coordinates reduce to $Z=(2n+1)D$ and $-(2n-1)D$ for $n=1,2,3\ldots$ With this optical insight, it is now possible to build up a system of electrostatic images to yield a potential function for V_1, which will

satisfy the equations of the previous section term by term.

In Chapter VII it will be shown theoretically that the symmetric case is favoured energetically (see figure 3) thus agreeing with experiment (7). Since the algebra is simpler for the symmetric case, that is $\beta = \frac{1}{2}$, the potential will be evaluated in the first instance assuming central location of the charge (d=D) and later generalised as the need arises.

If in figure 1(a) e^* be located at (0,0,D), its contribution to the potential in region W will be

$$V_1 = e^* K_w^{-1} \left[(z-D)^2 + y^2 + x^2\right]^{-\frac{1}{2}} \qquad \text{IV-(6)}$$

Successive images will be located at 0,0,-(2m-1)D and 0,0,(2m+1)D for m=1,2 ... On denoting $(K_w - K_g)(K_w + K_g)^{-1}$ by α, Jeans' (18) equations 129 and 131 for the relation between the tangential components of electric field at the boundary of a dielectric slab, can be generalised for successive reflections of charge and images in the system under consideration as

$$(\alpha^m + \alpha^{m+1})e^* = 2(K_w + K_g)^{-1} K_w \alpha^m e^* \qquad \text{IV-(7)}$$

for m=0,1,2 ...

There is correspondence between n in the exponent of α, and in the coordinates of the images contributing to the field in region W. That is, for any n=1,2 ..., images of charge $\alpha^n e^*$ are located at $[0,0,-(2n-1)D]$ and $[0,0,(2n+1)D]$ respectively. Since α is always less than unity, the potential due to each set of images forms a convergent series and hence is finite. We may say the sets are enumerable.

It is now possible to make an informed guess at the potential in regions W, M_1 and M_2, and then fit the assumed expressions to the boundary conditions. By assumption the contribution of V_1 to the potential in W, M_1 and M_2 will be harmonic functions, satisfying the Laplace equation everywhere except at (0,0,D) (remember we have agreed for the moment that d=D) the location of the charge or source, where it satisfies equation IV-(2). If the boundary conditions given in section 4 are also satisfied, then such a potential function represents a solution to the problem but for a constant.

Proceeding in this manner, the contribution of the images to the potential in region W may be written as

$$V_2+V_3=\frac{e^*}{K_W}\left[\sum_{n=1}\frac{\alpha^n}{\{[z+(2n-1)D]^2+y^2+x^2\}^{\frac{1}{2}}}+\sum_{n=1}\frac{\alpha^n}{\{[z-(2n+1)D]^2+y^2+x^2\}^{\frac{1}{2}}}\right]$$

IV-(8)

On taking surfaces into account, it should be noted that the slab occupying the region $Z < 0$, sees the images located at $[0,0,(2n+1)D]$, where $n=1,2 \ldots$ as virtual charges. The reverse is true for the slab at $Z > 2D$. Thus for the contribution of V_1 to the potential in M_1 we have from equation IV-(7)

$$V_{M_1} - V_F = 2e^*(K_W+K_M)^{-1} \sum_{n=0} \{[z-(2n+1)D]^2+y^2+x^2\}^{-\frac{1}{2}} \qquad \text{IV-(9)}$$

and for M_2

$$V_{M_2} - V_F = 2e^*(K_W+K_M)^{-1} \sum_{n=0} \{[z+(2n-1)D]^2+y^2+x^2\}^{-\frac{1}{2}} \qquad \text{IV-(10)}$$

It can be easily shown that if we write

$$V_W - V_F = V_1 + V_2 + V_3 \qquad \text{IV-(11)}$$

then equations IV-(9), -(10), -(11) which represent V_1 in regions M_1, M_2 and W respectively, satisfy all the requirements demanded in section 1.

In order to get a complete solution, the following relations must hold:

$$V_W = V_{M_2}$$

$$-K_W \frac{\partial V_W}{\partial z} + K_M \frac{\partial V_{M_2}}{\partial z} = -4\pi\sigma \qquad \text{IV-(12)}$$

at $z=2D$ and

$$V_W = V_{M_1}$$

$$K_W \frac{\partial V_W}{\partial z} - K_M \frac{\partial V_{M_1}}{\partial z} = -4\pi\sigma \qquad \text{IV-(13)}$$

at $z=0$

These conditions can be satisfied by choosing V_σ according to the following scheme

$$V_\sigma = \frac{4\pi\sigma z}{K_M} \qquad -\infty < z < 0$$

$$= 0 \qquad 0 < z < 2D \qquad \text{IV-(14)}$$

$$= \frac{4\pi\sigma(2D-z)}{K_M} \qquad 2D < z < \infty$$

Strictly speaking since the slabs are only effectively infinite ∞ should be replaced by a cut-off planes $z=-L$ and $z=2D+L$, such that V_σ vanishes for $z<-L$, $z>2D+L$ and also $D<L$. The z coordinate L therefore represents an unknown singular point, where the slabs in regions M_1 and M_2 cease to be effectively infinite in the place z=constant. This matter is discussed more fully in the next section and a possible solution explored in Chapter VII. It should be stressed however, that what is really meant by the scheme for V_σ, is that in the neighbourhood of the surfaces z=0 and z=2D, the contribution of the surface charge to the potential in the regions M_1, M_2 and W can be described by the expressions given for V_σ in IV-(14).

It is well to note, that unlike a condenser, the field due to the surface charge, at z=0 and z=2D is set uniform over the separation 2D. A little reflection will show, that if the real charges were absent, the free surface charge on the slabs would be sinks for sources at infinity. The choice of V_σ is such that the force on a test charge located at z=D, due to V_σ vanishes, as would be expected from symmetry considerations. This is also support for selecting the central position.

The changes required to generalise V_W-V_σ , for

$\beta \neq \frac{1}{2}$, are quite simple yielding

$$V_W - V_\sigma = \frac{\sigma^2}{\epsilon_W}\left[\frac{1}{\{(z-d)^2+y^2+x^2\}^{\frac{1}{2}}} + \sum_{n=0} \frac{\alpha^{2n+1}}{\{(z+4nD+d)^2+y^2+x^2\}^{\frac{1}{2}}}\right.$$

$$+ \sum_{n=0} \frac{\alpha^{2n+1}}{\{(z-(4n+1)D+d)^2+y^2+x^2\}^{\frac{1}{2}}} +$$

$$+ \sum_{n=0} \frac{\alpha^{2n+2}}{\{(z+4(n+1)D+d)^2+y^2+x^2\}^{\frac{1}{2}}}$$

$$\left. + \sum_{n=0} \frac{\alpha^{2n+2}}{\{(z-4nD-d)^2+y^2+x^2\}^{\frac{1}{2}}}\right] \qquad \text{IV-(15)}$$

(n+1)

$V_{M_1} - V_\sigma$ and $V_{M_2} - V_\sigma$ can be derived from equation IV-(15) without difficulty.

The reader may at this stage, prove for himself, that the method of images breaks down for model II, since the regions are multiply dis connected.

3. Models I and II via Fourier Transform Methods

In this development the discontinuity in the normal component of the electric displacement, will be

removed once and for all by selecting V_σ in such a way that only V_1 remains to be determined. Three choices will therefore be made for ψ in the respective models I, II(a) and II(b).

It can be readily verified that a suitable choice of ψ is given by the following expressions:

$$\begin{aligned}
\psi &= \beta\pi z/K_M && -\infty < z < 0, \\
&= 0 && 0 < z < 2D, \\
&= \beta\pi(2D-z)/K_M && 2D < z < \infty
\end{aligned} \qquad \text{IV-(16)}$$

$$\begin{aligned}
\psi &= \frac{\beta\pi(z+b)}{K_W} - \frac{\beta\pi b}{K_M} && -\infty < z < -b, \\
&= \frac{\beta\pi z}{K_M} && -b < z < 0, \\
&= 0 && 0 < z < 2D, \\
&= -\frac{\beta\pi(z-2D)}{K_M} && 2D < z < 2D+b, \\
&= -\frac{\beta\pi(z-2D-b)}{K_W} - \frac{\beta\pi b}{K_M} && 2D+b < z < \infty
\end{aligned} \qquad \text{IV-(17a)}$$

$$\begin{aligned}
\psi &= \frac{\beta\sigma\pi(z+b)}{K_W} - \frac{\beta\sigma\pi b}{K_M} && -\infty < z < -b, \\
&= \frac{\beta\sigma\pi z}{K_M} && -b < z < 0
\end{aligned}$$

$$= 0 \qquad 0 < z < 2D,$$

$$= \frac{-4\pi\sigma(z-2D)}{K_M} \qquad 2D < z < 2D+b,$$

$$= \frac{-4\pi\sigma(z-2D-b)}{K_W} - \frac{4\pi\sigma b}{K_M} \qquad 2D+b < z < \infty \qquad \text{IV-(17b)}$$

In the determination of V_p given here it has been assumed that the platelets are infinite in extent, so that the potential due to the surface charges tends to infinity as $z \to \pm\infty$. Physically this is of course not permissible, for when the finite extent of the platelets is taken into account the potential will tend to zero as $z \to \pm\infty$. The exact determination of the potential due to platelets of finite area is a much more complicated calculation, and so instead the following approximation is made. As the expressions given in equations IV-(16) and IV-(17) are still valid if the same constant is added to V_p over all space, if we add to the right hand side of IV-(16) a term $4\pi\sigma L/K_M$, and choose V_p to be zero from $z < -L$, $z > 2D+L$, we have a potential which varies linearly near the platelets, and is cut off from z sufficiently large positive or negative. The changes required in equations IV-(17a) and IV-(17b) are the addition of

$$\frac{8\pi\sigma(L-b)}{K_W} + \frac{4\pi\sigma b}{K_M} \quad \text{and}$$

$$\frac{4\pi\sigma(L-b)}{K_W} + \frac{4\pi\sigma b}{K_M} \quad \text{respectively,}$$

with $V_\sigma = 0$ for $z < -L$ and $z > 2D+L$.

In order to determine V_1 the method of Fourier transforms is used. This method is well adapted to problems with plane boundaries extending to infinity, and gives automatically the equivalent distribution of images. The following assumed forms for the potentials in models I and II are made (there is no difference between II(a) and II(b) now that the discontinuities have been incorporated in V_σ):

$$-V_\sigma + V_{M_1} = \frac{1}{2\pi i}\int_{-\infty}^{\infty} dk_1 \int_{-\infty}^{\infty} dk_2 \int_{c_-} dk_3 P^{M_1}(\underset{\sim}{k})\, \frac{e^{i\underset{\sim}{k}\cdot\underset{\sim}{x}}}{k^2},$$

$$-V_\sigma + V_W = \frac{\sigma}{2\pi^2 K_W}\int_{-\infty}^{\infty} dk_1 \int_{-\infty}^{\infty} dk_2 \int_{-\infty}^{\infty} dk_3\, \frac{e^{i\underset{\sim}{k}\cdot(\underset{\sim}{x}-2\underset{\sim}{b})}}{k^2}$$

$$+ \frac{1}{2\pi i}\int_{-\infty}^{\infty} dk_1 \int_{-\infty}^{\infty} dk_2 \left[\int_{c_+} dk_3 P_+^W(\underset{\sim}{k})\frac{e^{i\underset{\sim}{k}\cdot\underset{\sim}{x}}}{k^2} + \int_{c_-} dk_3 P^W(\underset{\sim}{k})\frac{e^{i\underset{\sim}{k}\cdot\underset{\sim}{x}}}{k^2}\right]$$

$$-V_0 + V_{M_2} = \frac{1}{2\pi i}\int_{-\infty}^{\infty} dk_1 \int_{-\infty}^{\infty} dk_2 \int_{C_+} dk_3 F^{M_2}(k)\, e^{i\underset{\sim}{k}\cdot\underset{\sim}{x}}$$

IV-(18)

for model I, and

$$-V_0 + V_{M_1} = \frac{1}{2\pi i}\int_{-\infty}^{\infty} dk_1 \int_{-\infty}^{\infty} dk_2 \int_{C_-} dk_3 F^{M_1}(\underset{\sim}{k})\, e^{i\underset{\sim}{k}\cdot\underset{\sim}{x}}$$

$$-V_0 + V_{M_1} = \frac{1}{2\pi i}\int_{-\infty}^{\infty} dk_1 \int_{-\infty}^{\infty} dk_2 \left[\int_{C_+} dk_3 F_+^{M_1}(\underset{\sim}{k})\, e^{i\underset{\sim}{k}\cdot\underset{\sim}{x}} + \int_{C_-} dk_3 F_-^{M_1}(\underset{\sim}{k})\, e^{i\underset{\sim}{k}\cdot\underset{\sim}{x}}\right]$$

$$-V_0 + V_{M_2} = \frac{E_0}{2\pi i x_M}\int_{-\infty}^{\infty} dk_1 \int_{-\infty}^{\infty} dk_2 \int_{-\infty}^{\infty} dk_3\, e^{i\underset{\sim}{k}\cdot(\underset{\sim}{x}-\underset{\sim}{x}_0)}$$

$$+ \frac{1}{2\pi i}\int_{-\infty}^{\infty} dk_1 \int_{-\infty}^{\infty} dk_2 \left[\int_{C_+} dk_3 F_+^{M_2}(\underset{\sim}{k})\, e^{i\underset{\sim}{k}\cdot\underset{\sim}{x}} + \int_{C_-} dk_3 F_-^{M_2}(\underset{\sim}{k})\, e^{i\underset{\sim}{k}\cdot\underset{\sim}{x}}\right]$$

$$-V_0 + V_{M_2} = \frac{1}{2\pi i}\int_{-\infty}^{\infty} dk_1 \int_{-\infty}^{\infty} dk_2 \left[\int_{C_+} dk_3 F_+^{M_2}(\underset{\sim}{k})\, e^{i\underset{\sim}{k}\cdot\underset{\sim}{x}} + \int_{C_-} dk_3 F_-^{M_2}(\underset{\sim}{k})\, e^{i\underset{\sim}{k}\cdot\underset{\sim}{x}}\right]$$

$$-V_\sigma + V_{W3} = \frac{1}{2\pi i}\int_{-\infty}^{\infty} dk_1 \int_{-\infty}^{\infty} dk_2 \int_{c_+} dk_3 P^W{}_3(\underset{\sim}{k}) \frac{e^{i\underset{\sim}{k}\cdot\underset{\sim}{z}}}{k^2}$$

IV-(19)

for model II. The symbols c_+ and c_- denote small circular contours in the complex k_3 plane taken in the anticlockwise sense and enclosing the poles of the integrand of the points $k_3 = \pm i\,(k_1^2 + k_2^2)^{\frac{1}{2}}$ respectively. The choice of these contours is such that the potentials have the correct behaviour as $z \to \pm\infty$. The vector z_0 has components $(0,0,d)$. The unknown functions $F(\underset{\sim}{k})$ are determined by substituting the expressions IV-(18) and IV-(19) in the boundary conditions IV-(3) and by requiring V_i to be continuous across the interfaces. From the uniqueness theorem for Fourier transforms these conditions may be expressed as a set of algebraic equations to determine the unknown functions. The solutions of these equations are:

$$P^W_+(\underset{\sim}{k}) = \frac{ie^*}{\varepsilon K_W \Delta}\left[(K_M^2 - K_W^2)e^{(4D-d)k} - (K_M - K_W)^2\, e^{dk}\right],$$

$$P^W_-(\underset{\sim}{k}) = \frac{ie^*}{\varepsilon K_W \Delta}\left[(K_M - K_W)^2 e^{-dk} - (K_M^2 - K_W^2)e^{dk}\right],$$

$$P^{M_1}(\underset{\sim}{k}) = \frac{2ie^*}{\varepsilon\Delta}\left[(K_M - K_W)e^{dk} - (K_M + K_W)e^{(4D-d)k}\right],$$

$$P^{M_2}(\underset{\sim}{k}) = -\frac{2ie^*}{\varepsilon\Delta}\left[(K_M + K_W)e^{(4D+d)k} - (K_M - K_W)e^{(4D-d)k}\right]$$

IV-(20)

for model I, and

$$F^{W_1}(\underline{k}) = \frac{4ie^2}{w\Delta_2} K_W e^{2bk}\left[e^{(4D-d)k} H + e^{dk} Z\right],$$

$$F_+^{M_1}(\underline{k}) = \frac{2ie^2(K_W-K_M)}{w\Delta_2}\left[e^{(4D-d)k} H + e^{dk} Z\right],$$

$$F_-^{M_1}(\underline{k}) = \frac{2ie^2(K_W+K_M)}{w\Delta_2} e^{2bk}\left[e^{(4D-d)k} H + e^{dk} Z\right],$$

$$-F_+^{W_2}(\underline{k}) = \frac{4e^2 Z}{w K_W \Delta_2}\left[e^{(4D-d)k} H + e^{dk} Z\right],$$

$$F_-^{W_2}(\underline{k}) = \frac{4e^2 Z}{w K_W \Delta_2}\left[e^{dk} H + e^{-dk} Z\right],$$

$$-F_+^{M_2}(\underline{k}) = \frac{2ie^2(K_W+K_M)}{w\Delta_2} e^{2(2D+b)k}\left[e^{dk} H + e^{-dk} Z\right],$$

$$F_-^{M_2}(\underline{k}) = -\frac{2ie^2(K_W-K_M)}{w\Delta_2}\left[e^{dk} H + e^{-dk} Z\right],$$

$$F^{W_3}(\underline{k}) = -\frac{4ie^2 K_M}{w\Delta_2} e^{2(2D+b)k}\left[e^{dk} H + e^{-dk} Z\right] \qquad \text{IV-(21)}$$

for model II. The following abbreviations have been used in equations IV-(20) and IV(21):

$$k = (k_1^2 + k_2^2)^{\frac{1}{2}};$$

$$\Delta_1 = (K_W-K_M)^2 - (K_W+K_M)^2 e^{-2bk}$$

$$R = (K_p+K_q)^2 e^{2bk} - (K_p-K_q)^2,$$

$$S = (K_p^2-K_q^2)(e^{2bk}-1)$$

$$\Delta_e = S^2 - e^{4bk} R^2 \qquad \text{IV-(22)}$$

4. General Extensions and the Equivalence of the two Methods

Various checks on the results of the previous sections, can be made by considering certain well known limiting cases. If for example $z=2b$, in the equations just derived for the potential for model I, we obtain the well known solution for a single point charge, in a medium with a single plane interface, namely:

$$V_{p_1} - V_e = \frac{2e^{-(K_p+K_q)-1}}{\{(z-d)^2+y^2+x^2\}^{\frac{1}{2}}} \qquad \text{IV-(23)}$$

$$V_p - V_e = \frac{e}{K_p}\left[\frac{1}{\{(z-d)^2+y^2+x^2\}^{\frac{1}{2}}} + \frac{\alpha}{\{(z+d)^2+y^2+x^2\}^{\frac{1}{2}}}\right]$$

$$\text{IV-(24)}$$

When $K_q \to \infty$, $\sigma=0$ in these same equations, we have the solutions for a point charge between two plane parallel conductors:

$$V_{p_1} = V_{p_2} = 0 = \text{a constant} \qquad \text{IV-(25)}$$

$$V_w - V_\sigma = \frac{e^{\beta}}{K_y \{(z-d)^2+y^2+x^2\}^{\frac{1}{2}}}$$

$$+ \frac{e^{\beta}}{K_y} \int_0^\infty dk\, J_0(kr)\, e^{-kz} \left\{ \frac{2e^{4D} \sin hd}{1-e^{-4Dk}} + \frac{(e^{d-4D} - e^{-d})}{1-e^{4Dk}} \right\}$$

IV-(26)

If the denominators in the second term are expanded in powers of $e^{\pm 4D}$ and integrated term by term, the resultant series corresponds to sets of images in which $\sigma = -1$ but with z coordinates the same as those in equation IV-(15). If the first term, that is the charge, is included under the integral sign, the expression in curly brackets becomes

$$\left\{ \frac{(e^{d-4D} - e^{-d})}{1-e^{4Dk}} + \frac{e^{d} - e^{4D-d}}{1-e^{-4Dk}} \right\}$$

and the z coordinates for images and charge become $d \pm 4mD$ and $-d \pm (4m+1)D$, $m=0,1,2 \ldots$ Equation IV-(26) can be extended by inversion to describe the potential of two conducting spheres in contact, whilst if $d=0$ it gives automatically the conditionally convergent potential for a symmetric one dimensional ionic crystal lattice.

When K_y is finite for any $\beta = d/2D$ we have for model I

$$V_W - V_\sigma = \frac{\rho^2}{K_W}\int_0^\infty dk\, J_0(kr)e^{-ks}\left\{\frac{(e^{d-4D}+\alpha e^{-d})}{1-\alpha^2 e^{-4Dk}} + \frac{(e^{d}+\alpha e^{4D-d})}{1-\alpha^2 e^{-4Dk}}\right.$$

IV-(27)

with similar expressions for $V_{M_1}-V_\sigma$ and $V_{M_2}-V_\sigma$.
Equation IV-(27) is of course equivalent to IV-(15).
Equations IV-(15) and IV-(27) for the case d=D reduce at once to

$$V_W - V_\sigma = \frac{\rho^2}{K_W}\int_0^\infty dk\, J_0(kr)e^{-ks}\left\{\frac{e^{D}}{1-\alpha e^{-2Dk}} + \frac{e^{-D}}{1-\alpha e^{-2Dk}}\right\}$$

IV-(28)

which is just IV-(11). There is no reason in principle why model I cannot be generalised for several sources in region W satisfying equation IV-(4). This is the actual situation in practice. Such a model would generate potential functions for a two dimensional lattice, taking into account any cross interactions which model I as it stands ignores. Methods* for computing such two dimensional lattice sums in the energy calculation will be given in Chapter V.

The limit of equation IV-(21) as $b \to \infty$, reduces to equation IV-(20) for model I as it should. Equation IV-(21) cannot be reduced completely to sets of images generated by repeated reflections, for if D/b were irrational such a set

*This matter has been explored for the case of two conducting interfaces by C.A. Barlow & J.R. MacDonald , J.Chem. Phys. 40, 1535 (1964).

would be everywhere dense. The potential derived from such a set of images would not be an analytic function in view of the everywhere dense set of singularities. A naive application of the method of images will not therefore give a satisfactory solution as discussed in II-2.*

5. Extension to Monolayers and Membranes

If in figure 1(b) we let $z=2D \to \infty$ thus eliminating regions R_2 and R_3, we have the desired model. The potential in region R_2 due to the ion and its images is simply:

$$V_{R_2} - V_0 = \frac{e^*}{K_w}\left[\frac{1}{\{(z-d)^2+y^2+x^2\}^{\frac{1}{2}}} + \frac{\alpha}{\{(z+d)^2+y^2+x^2\}^{\frac{1}{2}}}\right]$$

$$- \frac{e^*\alpha(1-\alpha^2)}{K_w}\int_0^\infty \frac{dk\, J_0(kr)\, e^{-k(z+d+2b)}}{1+\alpha^2 e^{-2bk}}$$

IV-(29)

*The method of Fourier transforms obviates this difficulty by selecting only the subset of images necessary to satisfy the boundary conditions and the differential equations. What seems to happen is that this method truncates the sets of images so as to isolate the singularities. For two interfaces the potential function due to the ion and its images has only one limit point, namely at infinity. The potential due to the images is analytic throughout the entire region and is zero at infinity. With the addition of more interfaces the image method multiplies the singularities and has no built in selection mechanism.

$$V_{s_1} - V_0 = 2e^2(K_w+K_m)^{-1}\int_0^\infty dk\, J_0(kr)e^{-kz}\,\frac{(e^{d} - \alpha_{23}e^{-d-2b})}{1-\alpha^2e^{-2bk}}$$

$$+ \quad 2e^2\alpha\ (K_w+K_m)^{-1}\left[\ \frac{1}{\{(z+d)^2+y^2+x^2\}^{\frac{1}{2}}}\ \right]$$

IV-(30)

$$V_{s_1}-V_0 = \frac{e^2}{K_w}(1-\alpha^2)\int_0^\infty \frac{dk\, J_0(kr)\ e^{(d-z)k}}{(1-\alpha^2e^{2dk})} \qquad \text{IV-(31)}$$

It is well to note, that if we regard regions s_2, s_1, s_1 as regions 1,2,3 having dielectric constants K_1, K_2, K_3 and define $\alpha_{ij} = (K_i-K_j)(K_i+K_j)^{-1}$; we get the useful general case for a single uncharged monolayer, with perhaps a liquid on the underside and air on the outer. For such a situation we have for the potential in regions 1,2, and 3 the following:

$$V_1' = \frac{e^2}{K_1}\left[\ \frac{1}{\{(z-d)^2+y^2+x^2\}^{\frac{1}{2}}} + \frac{\alpha_{12}}{\{(z+d)^2+y^2+x^2\}^{\frac{1}{2}}}\ \right]$$

$$+ e^2\alpha_{23}\,\frac{(1-\alpha_{12}^2)}{K_1}\int_0^\infty \frac{dk\, J_0(kr)e^{-k(z+d+2b)}}{1-\alpha_{12}\alpha_{23}e^{-2bk}}$$

IV-(32)

$$V_2' = 2e^2(K_1+K_2)^{-1}\int_0^\infty \frac{dk\, J_0(kr)e^{k(d-z)}}{1-\alpha_{zs}\alpha_{sz}e^{-2bk}}$$

$$+ 2e^2\alpha_{1s}K_3(K_2+K_3)^{-1}K_1^{-1}\{(z+d)^2+y^2+x^2\}^{\frac{1}{2}}$$

$$+ 2e^2(K_1+K_2)^{-1}\sum_{n=1}^{\infty}\alpha_{zs}^{n}\alpha_{sz}^{n-1}\{(z+d+2nb)^2+y^2+x^2\}^{\frac{1}{2}}$$

IV-(33)

$$V_3' = \frac{e^2}{K_1}(1+\alpha_{zs})(1+\alpha_{1s})\int \frac{dk\, J_0(kr)e^{(d-z)k}}{1+\alpha_{1s}\alpha_{sz}e^{2bk}}$$

IV-(34)

Equations IV-(32), -(33), -(34), are sufficient to discuss the behaviour of a single uncharged monolayer or membrane. If a knowledge of V_o is available, a scheme can be developed as in the previous section.

If there is a compound membrane or an array of slabs, the problem becomes much more complicated. Of course this is usually the actual situation in biological tissue or even returning to the case of the platelets of montmorillonite arranged to form a crystal. One way out, is to use equation IV-(32), noting that the first two terms will always reduce to case of a single plane interface

IV-(23) and IV-(24). Surely would the situation demand attempting to follow through the laborious algebra, which a more complicated model would entail. Perhaps a suitable generator function may be the answer.

Although the developments represented by the potential functions contain all the information necessary to discuss the properties of the various models, they are not very convenient. What is required is the potential energy or energy of interaction.

CHAPTER V

EVALUATION OF ELECTROSTATIC ENERGY OF INTERACTION

1. Model I via Image Methods

By the aid of Green's theorem, the energy of the electric field, $(\vec{\nabla}V)$ in any region of three dimensional space, can be expressed as a surface integral, as follows:

$$U_E = \frac{1}{8\pi}\iiint K(\nabla V)^2 \, dx\,dy\,dz = -\frac{1}{8\pi}\sum_i \iint KV \frac{\partial V}{\partial n_i} \, ds_i \qquad V-(1)$$

where s_i is the i^{th} surface of dielectric or conductor in the region and $\frac{\partial V}{\partial n_i}$ the normal derivative from the surface into the region. It may be noted that $-\frac{1}{4\pi}\frac{\partial V}{\partial n_i}$, is just σ_i, the surface density of charge (bound or free) over the i^{th} surface. To evaluate the energy for regions W, M_1 and M_2, all that is necessary in principle is to substitute V_W, V_{M_1}, V_{M_2} in equation V-(1) and carry out the integrations indicated for the various regions. Thus we shall obtain

$$U_E = U_W + U_M \qquad V-(2)$$

where $U_M = U_{M_1} + U_{M_2}$.

Before writing out U_W and U_M in full, simplifications may be made in computing the interaction energy. It is possible to eliminate self energy terms and terms involving the surfaces of images. The latter being fictitious are indeed zero.

The self energy terms are independent of the location of the interfaces and since we are interested in the potential energy it does not interest us except to set the zero of energy. After doing this, the significant interaction energy terms will be those arising from the following cross terms.

(a) The real charge with all the images contributing to the potential in region W.

(b) The images with the free charge on the surfaces z=0 and z=2D.

(c) The real charge with the free charge on the surfaces z=0 and z=2D.

(d) Interaction between the free charge on the surfaces z=0 and z=2D.

The terms (c) and (d) represent the purely Coulombic terms as opposed to the polarization terms (a) and (b). In computing (c) and (d) it should be observed from equations IV-(25) and IV-(26) that the expressions for V_σ do not carry over in the case of a conductor. It would appear therefore that an exact solution for the potential and energy between two negative plates is not

possible by these methods. The best approximation seems to be to change the zero of the potential due to V_σ by adding $4\pi\sigma D/K_W$ to IV=(14) and IV-(17b) and $8\pi\sigma D/K_W$ to IV-(17a). These constants have been obtained by the superposition of the potential due to effectively infinite sheets of charge.

Finally we may note that (b) may be separated into contributions from sets image charges describing the potential in the different regions. This is useful since it facilitates comparison with thermodynamic data on the free energy change of both substances.

On carrying out the appropriate integrations and putting $e^* = ze$, we obtain

$$U_W = -\frac{z^2e^2}{2DK_W}\ln(1-\alpha) + \frac{2\pi\sigma ze}{K_W+K_M}\sum_{n=0}^{\infty}\alpha^n\left[\left\{(2n+1)^2D^2 + ze/2\pi\sigma\right\}^{\frac{1}{2}} - (2n+1)D\right] + \frac{2\pi\sigma zeD}{K_W} \quad \text{ergs/ion} \qquad \text{V-(17)}$$

and

$$U_M = \frac{2\pi\sigma ze}{K_W+K_M}\sum_{n=0}^{\infty}\alpha^n\left[\left\{(2n+1)^2D^2 + ze/2\pi\sigma\right\}^{\frac{1}{2}} - (2n+1)D\right] \quad \text{ergs/ion} \qquad \text{V-(14)}$$

In view of the discussion following equation IV-(14) we must have for large values of 2D.

$$U_W = \frac{-z^2e^2}{2DK_W}\ln(1-\alpha) + \frac{2\pi\sigma ze}{K_W+K_M}\sum_{n=0}^{\infty}\alpha^n\left[\left\{(2n+1)^2D^2 + ze/2\right\}^{\frac{1}{2}} - (2n+1)D\right] \qquad \text{V-(18)}$$

Similar but more laborious computations can be carried out when $\beta \neq \frac{1}{2}$ using equation IV-(15) in place of IV-(11).

From the view point of the industrial chemist, biologist or engineer all he requires are equations V-(14), -(1 and -(18) to discuss the general stability behaviour of condensed systems consisting of plate-shaped particles.

2. Models I and II via Fourier Transform Methods

As shown in section 1 the total energy in the field is given by

$$U = \frac{1}{8\pi} \iiint K(\nabla V)^2 \, dx\,dy\,dz \qquad V-(19)$$

where the integration is carried out over the whole three dimensional space. In this problem the dielectric constant is a function of coordinates in a manner to be described in Chapter VI. Actually it is piecewise constant. By the use of Green's theorem, equation V-(19) may again be expressed as a surface integral

$$U = \tfrac{1}{2} e\, V(0,0,d) + \tfrac{1}{2} \sum_i \sigma_i \int_{S_i} V_i \, dS_i - \frac{1}{8\pi} \int_{z=-\infty} KV \frac{\partial V}{\partial z} \, ds$$

$$+ \frac{1}{8\pi} \int_{z=+\infty} KV \frac{\partial V}{\partial z} \, ds \qquad V-(20)$$

where $z = \pm_\infty$ are fictitious surfaces.

When computing the total energy of the field, it must be borne in mind that the parameter D is to vary, and hence the fictitious surfaces $z = \pm_\infty$ should be replaced by surfaces whose coordinates are independent of D. Suitable choices are $z = \pm L'$ where L' is at a fixed distance from the origin.

The surfaces $z = \pm L'$ are chosen such that they are near to $z = -L$ and $z = 2D+L$ without coinciding with them. The proper incorporation of this very important contribution to the energy requires an exact treatment of edge effects associated with finite platelets to be attempted in Chapter VII. We have also ignored the self energy of the ion, which is independent of its location, that is stationary with respect to coordinates. Using equations IV-(16) to -(22) we find U_R for the various models chosen:

$$U_R = \frac{\alpha (e^*)^2}{9DK_W} \int_0^\infty \frac{dx}{x} \frac{x^2 + 2_p x + x^{1-p}}{1 - \alpha^2 x}$$

$$+ \frac{2e^2 \alpha_{M-W}}{K_W + K_M} R \int_0^\infty \frac{dk}{k} J_1(kR) \frac{e^{\frac{dk}{Dk} + \alpha} (2D-d)k}{e^{Dk} - \alpha}$$

$$- \frac{4\pi^2 e^2 R^2 D}{K_W} + \frac{4\pi^2 e^2 R^2 (L'-L)}{K_M} + \frac{2\pi e^2 L}{K_M} \qquad V-(21)$$

for model I. The terms which depend on L and L' have no physical significance and only serve to set the zero of U. In computations only the D dependent part of the surface-surface interaction energy is considered.

For model II we have

$$U_E = \frac{\alpha(e^2)^2}{4DK_W} \int_0^1 \frac{dx}{x} \frac{(1-x^\gamma)(1-\alpha^2 x^\gamma)(x^\beta + x^{1-\beta}) + 2\alpha x(1-x^\gamma)}{(1-\alpha^2 x^\gamma)^2 - \alpha^2 x(1-x^\gamma)^2} + U_E'$$

where

$$U_g' = -2e^2\sigma\pi R(K_W+K_M)\int_0^\infty \frac{dk}{k} J_1(kR)\,\frac{(e^{bk}+1)(e^{bk}-\alpha)(e^{dk}+e^{(2D-d)k})}{2-e^{2Dk}\,\Pi}$$

$$-\frac{16\,\pi^2\sigma R^2 D}{K_W} \qquad \text{V-(22a)}$$

for model IIa and

$$U_g' = -2e^2\pi\sigma R(K_W+K_M)\int_0^\infty \frac{dk}{k} J_1(kR)\,\frac{(e^{2bk}-\alpha)(e^{dk}+e^{(2D-d)k})}{2-e^{2Dk}\,\Pi}$$

$$-\frac{4\,\pi^2\sigma R^2 D}{K_W} \qquad \text{V-(22b)}$$

for model IIb. The D-independent surface-surface terms have been dropped. The notation used in these equations is

$$\alpha = \frac{K_W-K_M}{K_W+K_M}\,, \quad \beta = \frac{d}{2D}, \quad \gamma = \frac{b}{2D}$$

and x is a dummy variable.

In the calculation of equations V-(21) and V-(22) further approximations have been made. As mentioned before the total field, and hence the total energy, of an infinite plane interface with a uniform charge density is infinite, so we have introduced a cut off radius R, and the total area

of interaction per ion of a platelet is $A = \pi R^2 = e^2/2\sigma$. Physically this means that we are calculating the energy per ion, and we suppose that each ion in the region between two platelets interacts with such an amount of surface charge ($= \sigma A$ on each platelet that $e=2\sigma$. In other words each ion charge is just neutralised by the surface charge. There may be several ions per platelet pair, and in this case we suppose that each ion has its own separate region of influence, and we neglect interactions between neighbouring ions. This treatment should give the best results for ions of highest charge because the condition that each ion commands a region whose total charge just neutralizes that of the ion means that the higher charged ions are more sparsely distributed.

Inspection of the energy expressions V-(21) and V-(22) reveals that they all possess both a minimum and a maximum. For as $D \to 0$, the first term, describing the ion-image energy, diverges like D^{-1} and is positive, whilst the second term, in each case, tends to a finite value. The surface-surface term is proportional to D and so tends to zero. Hence for small D, W is large positive ... there is a repulsion at short distances. As $D \to \infty$, the first two terms, representing the contribution to the energy due to the presence of the ion, tend to zero. This is natural for

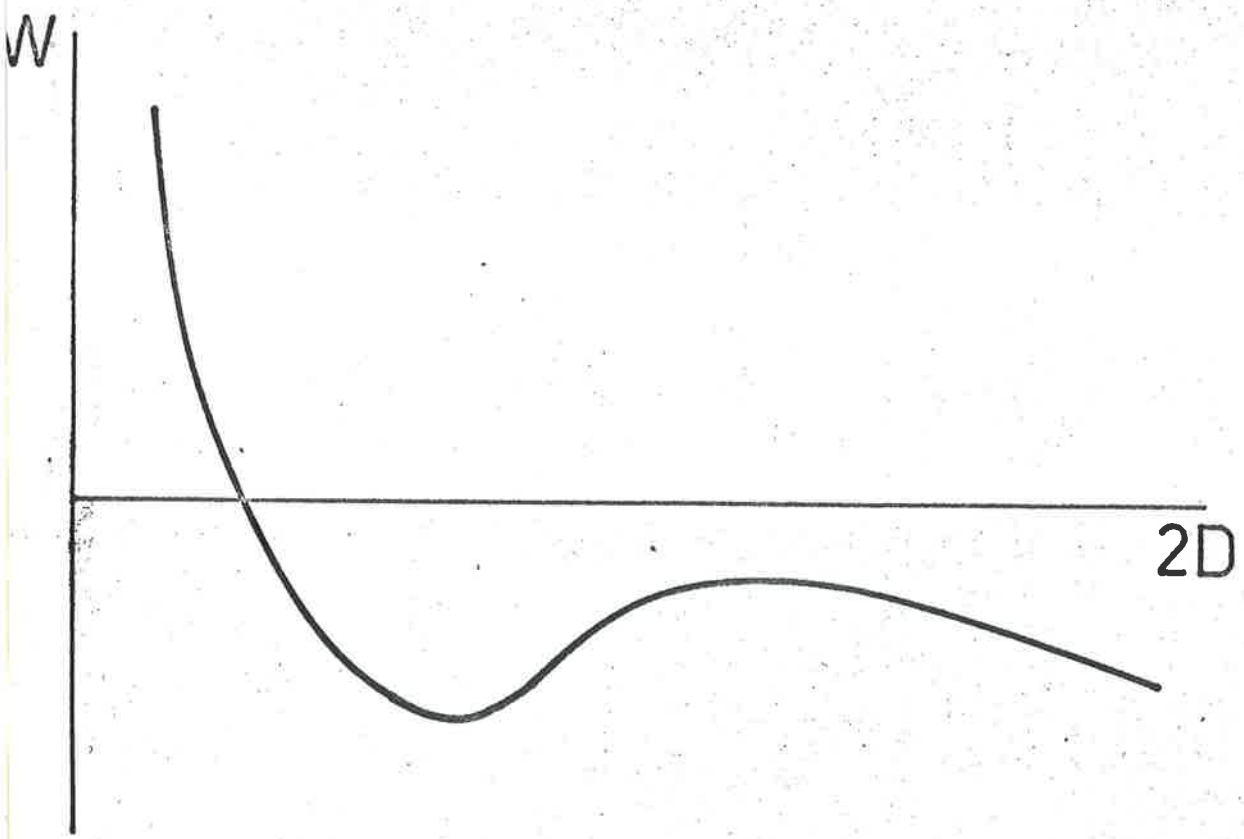

Fig. 2 General Behaviour of Electrostatic Energy as a Function of Platelet Spacing 2D

if the platelets are far apart they would have little effect on the ion. The surface-surface term becomes large negative, and decreasing, representing a repulsive force but is finally cut off as D->L. Hence there is the possibility of two minima. (See Chapter VII).

Calculations to be described in detail later, show that in the intermediate range the ion-surface charge energy which is attractive dominates and gives an attractive force. The general behaviour of the energy is shown schematically in figure 2. From experiments over the years such a curve is the one expected, for example (26, figure 9).

3. General Extensions and Influence of Excess Electrolyte

It may be noted that if the first terms only in the image series are taken equation V-17 reduces to

$$U_W = \frac{\alpha z^2 e^2}{-2DK_W} + \frac{2ze\pi\sigma}{K_W+K_M}\left\{D^2 + ze/2\pi\sigma\right\}^{\frac{1}{2}} - D + \frac{2ze\pi\sigma D}{K_W} \qquad V-(23)$$

This is the first order approximation and is the correct of (20, equation 8) given in an earlier work (20).

If now in figure 1(a) we replace regions M_1,

H_2 by two uncharged conducting plates, the potential in W is given by equation IV-(26). The energy of interaction is at once

$$U_W = - \frac{(e^*)^2}{2DK_W} \ln 2 \qquad V-(24)$$

which is of the form of a one dimensional ionic lattice sum with the ions a distance 2D apart. Equation V-(24) can also be used to estimate the potential energy when two conducting spheres having radius proportional to $(2D)^{-1}$, are in contact. It is doubtful whether this is of much value in considering spherical macromolecules, nonetheless equation V-(24) can be generalised with reservations as

$$U_W = - \frac{(e^*)^2}{2DK_W} \ln(1-\alpha); \quad |\alpha|<1 \qquad V-(25)$$

If now we consider the two dimensional lattice sum for the image ion interaction, that is when several ions are present in region W, with coordinates $(0,0,D)$ $(0,\pm 2R,D)$ ... $(0,\pm 2nR,D)$, the energy per ion is

$$\frac{(e^*)^2}{K_W} \left\{ \sum_{n=0}^{\infty} \alpha^n \left[\int_0^{\infty} \frac{dk\ J_0(k\pm(n))}{e^{kk}-t} \right] + \frac{\alpha}{2D} \int_0^{\infty} \frac{dk}{e^k - \alpha} \right\}$$

V-(26)

The ion-ion interaction is of course an infinitely large positive constant independent of D. The case of a true two dimensional ionic square lattice with R=D is given by

$$\frac{(e^*)^2}{RK_T}\left\{\sum_{n=1,m=0}(-1)^{n+m}\left(\int_0^\infty \frac{dk\ J_0(k\sqrt{n})}{e^k-1}\right) - \ln 2\right\} \qquad V\text{-}(27)$$

When R≠D we have for a rectangular ionic lattice

$$\frac{(e^*)^2}{RK_T}\left\{\sum_{n=1,m=0}(-1)^{n+m}\left(\int_0^\infty \frac{dk\ J_0(k\sqrt{nD})}{e^{Rk}-1}\right) - \frac{(R+D)}{2D}\ln 2\right\} \qquad V\text{-}(28)$$

Equations V-(27) and V-(28) are obviously not absolutely convergent as is equation V-(26). To satisfy himself the reader may arrange the terms as in a regular determinant and compute a few terms.*

---

* Again the reader is refered to Barlow and MacDonald J.C.P. 40, 1535 (1964).

does not affect the total magnitude of the energy. Moreover we can always work through and separate the expressions.

The influence of excess electrolyte deserves some comment in regard to model II which is the more realistic model. If regions W_1 and W_3 in figure 1(b) consist of dissolved salt in water, the Fourier transform method may still be applied if certain conditions can be satisfied. Perhaps the simplest case is to regard the medium in W_1 and W_3 as a dielectric continuum with an effective dielectric constant, suitably adjusted for electrical saturation effects. This is just the extension outlined in Chapter IV, section 4. The second case is to prescribe or evaluate a volume density of charge which is a function of z only. In the light of the planes z= -b, z=2D+b being infinite in extent, having a uniform charge distribution and with W_1 and W_3 extending to infinity, this assumption may be justifiable. This second case appears to be related to the so-called double layer theory. It may be shown later, that double-layer theory may be used for regions between adjacent piles of plates. For example between adjacent crystals of a montmorillonite sol, but not always between platelets within a given crystal.

We will now consider these two extensions, the problem is one of algebra and computation only.

Let us suppose that the regions W_1 and W_2 have a constant dielectric constant K_W, that W_1 and W_3 have a constant dielectric constant K_W^0 independent of the ion position, whilst W_2 has a dielectric constant $(K_W)_{av}$ as defined in equation VII-(1). The problem for model II can be set up as before with the difference that K_W in W_2 differs from that in W_1 and W_3. The solution is now the same as given in equation IV-(21) except that K_W where it appears explicitly is to be interpreted as K_W^0, and the abbreviations given in equation IV-(22) now mean the following:

$$R = (K_W^0+K_M)(K_W+K_M)e^{2bk} - (K_W^0-K_M)(K_W-K_M),$$

$$S = (K_W^0+K_M)(K_W-K_M)e^{2bk} - (K_W^0-K_M)(K_W+K_M) \qquad V-(29)$$

The symbol K_W in equation V-(29) stands for $(K_W)_{av}$. The energy expressions are replaced by

$$U_E = \frac{e^2}{bDK_W}\int_0^t \frac{dx}{x}\ \frac{(\alpha-\alpha_0 x^\gamma)[(1-\alpha\alpha_0 x^\gamma)(x^\beta+x^{1-\beta})+2x(\alpha-\alpha_0 x^\gamma)]}{(1-\alpha\alpha_0 x^\gamma)^2 - x(\alpha-\alpha_0 x^\gamma)^2} + U_E'$$

$$V-(30)$$

where α_0 is the same as α except that K_W is replaced by K_W^0 and U_E' is given by the following expressions:

$$U_g' = -2\pi r_0 R(K_w^0 + K_g) \int_0^\infty \frac{dk}{k} J_1(kR) \frac{(e^{2bk} - a_0)(e^{dk} + e^{(2D-d)k})}{2 - e^{2Dk} a_0} \qquad V-(30a)$$

for model II(a), and

$$U_g' = -2\pi r_0 R(K_w^0 + K_g) \int_0^\infty \frac{dk}{k} J_1(kR) \frac{(e^{bk} + 1)(e^{bk} - a_0)(e^{dk} + e^{(2D-d)k})}{2 - e^{2Dk} a_0} \qquad V-(30b)$$

for model II(b). Obviously model I is unaffected. Computations with equation V-(30b) instead of V-(22b) show, as expected, that there is little difference between the results, although for model II(a), the energy calculated from equation V-(22a) is about 50% lower than that calculated from V-(30a) for D small, but for D large the difference is much smaller, and the points of unstable equilibrium only differ by at most $1A^0$ in the two cases. Actually computations based on equations V-(30) are not more time consuming than those based on equations V-(22).

It is expected that within limits the general influence will be such that the smaller the value of K_w^0 the lower the energy or the more stable the system. Making use of figure 2 we expect a deeper minimum as calculations show.

In discussing the stability situation from the view point of a volume density, it must be borne in mind that seldom are two platelets found as depicted in figure 1(b). If we return to the original statement of the problem in Chapter III, section 1, model II(b) is to simulate the actual situation where an array of five to ten plates interact to form a crystal. In other words the expressions derived here for model II(b) would simulate the relations between any two platelets within the crystal. We shall therefore extend the influence of a volume density of charge in regions W_1 and W_3, to that which would maintain in similar regions outside a grouping of platelets or a crystal.

If there are few groupings, such that regions W_1 and W_3 may be assumed to be infinite in the direction of z, it seems feasible that the conventional approach using Boltzmann's theorem may be applied to determine the charge density in W_1 and W_3. Having obtained the density function we could then compute the interaction with regions R_1, W_2, R_2.

In order to illustrate the nature of the forces involved, consider that for model II(b), figure 1(b), a point charge is located at some point $(0,0,z)$ $z > 2D+b$ facing the slab $2D<z<2D+b$. This is just the type of

problem we have already considered in Chapter IV, section 5, and hence we expect a similar type of potential function to IV-(29), -(30) and IV-(31). It is not difficult to show, that if the energy is given by $\frac{1}{2}eV(0,0,z)$, and since a is invariably less than unity, an expression of the type given in equation IV-(29) would yield a repulsive force until equilibrium were attained. This force would be somewhat similar to that derivable from the first terms of equation V-(22). By virtue of the symmetry of the system, similar arguments hold for a point charge located at $z<0$. We may regard this system of forces, for several such point charges in regions W_1, W_3 as a constant image pressure tending to confine region W_2 in the case of figure 1(b). Extended to an array of slabs or a montmorillonite crystal, this pressure tends to reduce the tendency of platelets to increase their interlayer spacing 2D.

From the view point of the potential energy of the two slabs in figure 1(b), the image pressure may be regarded as a tension, and hence yields a negative term to the energy. This will lower the minimum in figure 2.

Suppose now, regions W_1 and W_3 do not extend to infinity, but that there is a similar array of slabs.

say at x coordinates such that x= -L" and x=2D+L", with -L"+b and 2D+L"-b being considerable distances. If the volume density of charge in V_1 and V_3 is not too great, we may now attempt to use conventional double-layer theory in addition to image forces to obtain the interaction energy. It is well known that double-layer theory yields a repulsive force, but from the view point of the stability of the array of slabs this is a tension and hence adds an attractive term to the energy.

Following this, we can modify the extensive calculations of Verwey and Overbeek (3) for our use in between neighbouring arrays of slabs, by simply reflecting their potential energy curves across the abcissa.

Of course it is still questionable in the author's mind, whether features like ζ potential and density, are not purely hydro-kinetic effects. In other words, a macroscopic volume density of charge, cannot be really defined for a condensed colloid system at rest. Perhaps therefore, the first method of a saturated dielectric continuum might suffice.

Actually we have so far under estimated the

power and generality of the image treatment for symmetric systems. If the excess electrolyte is to be considered as a volume density of charge which is a function of z only, say g(z) and be of exponential order, then the solution is straightforward if there is no free charge on the surface. From the symmetry of the system, we expect g(z) to be of exponential order and this is indeed the situation when the Boltzmann's theorem is used to determine g(z). For example if we consider the conventional density function used in double-layer theory we have from Verwey and Overbeek (33, p. 24, 2a; $\rho = -2nve \sin h (ve V/kT)$).

Actually they (33) have ignored the dielectric properties of the macromolecule. To rectify this situation we propose that for a single double-layer their equation (2a) (33, p. 24) be replaced by

$$\rho = -2nve \sin h (ve V(z)/kT) - e2nve \sin h (ve V(-z)/kT)$$

V-(31)

In the case of a single plane interface say z=0 and let z=2D→ ∞ in figure 1(a) we now replace the right hand side of equation IV-(2) by the above expression to obtain the potential in W. Similarly we choose $\rho = -k_W(K_W+K_M)^{-1}nve \sin h (ve V(z)/kT)$ for region M_1 and demand that the boundary conditions described in

Chapter IV section 1 be satisfied. Finally with a little effort, we may consider a second interface say s=20 with the same infinite reflection technique used in Chapter IV.

With these changes the Boltzmann theorem used in (33) could still be used to get a more meaningful solution.

This matter is pursued further in the appendix.

4. Case of Monolayers and Membranes

The energy relations to discuss these systems have already been alluded to in the previous section. The influence of charges next to membranes on monolayers is to produce image forces. These forces may contribute to give the surface pressures or positive forces which are known from experiment*. For uncharged monolayers these forces are independent of electrolyte concentration.

To see that these forces are invariably pressures we can apply equation V-(20) to IV-(32), to give for the energy of interaction per charge e* located at (0,0,d), the expression

---

* The references are too numerous to list but the reader is referred to Colloidal Surfactants by K. Shinoda et al., Academic Press (1963) New York, London.

$$U_1 = -\frac{a}{4\pi K_1}\frac{(e^*)^2}{d^4} + \frac{(e^*)^2}{2K_1}(1-\alpha_{12}^2)\int_0^\infty \frac{dk\, J_0(kr)e^{-2k(d+b)}}{1-\alpha_{12}\alpha_{23}e^{-2bk}} \qquad V-(32)$$

Equation V-(32) defines a path of decreasing energy with distance so long as $K_1 > K_2$, and the force $\left[-\frac{\partial U_1}{\partial d}\right]$ is undoubtedly positive, that is repulsive and clearly a pressure.

There is no reason why this treatment cannot be applied to a distribution of counter ions in region 1. As a first approximation, assume a uniform distribution and develop a two dimensional crystal lattice theory of images as in equation V-(26); on the other hand, one may seek a distribution function for the volume density as outlined in the section 3 of this chapter. Again the author expresses his reservations, with regards to a macroscopic volume density of charge distribution for condensed systems at rest.

If the assumptions concerning independent interactions are resorted to, one may simply estimate the number of charges per area in a plane facing the monolayer or membrane, and estimate the surface pressure to a first approximation with the aid of equation V-(32).

The developments presented here about monolayers are only exploratory and should be regarded as at most

qualitative. It is designed only to stimulate interest in this mode of approach.

The contribution of the energy terms we have just discussed to the surface energy of the monolayer is usually obscured by the much higher energy of cohesion of the molecules composing the monolayer. Actually in the case of ionized monolayers expressions like V-(26) to V-(28) could perhaps be modified to describe the interactions between the ionized molecules. The two dimensional lattice would now be the plane of the ionized monolayer, that is, z=constant.

CHAPTER VI

MECHANISTIC ASPECT OF STABILITY IN RELATION TO SPECIFIC ION EFFECT AND DIELECTRIC SATURATION

1. Mechanism of Swelling and Role of Hydration Energy of the Interlayer Ions

In all the models so far we have considered only fictitious point charges interacting with slabs of dielectric. It is now necessary that we proceed to the next step and consider the specific properties such as size and charge of these counter ions. The stability relations to which the energy expressions will be applied, can only be understood if there is some theory, as to the mechanism of the process for plate-shaped macromolecules. Thus for example before the stability of colloidal montmorillonite can be understood, we must understand the process, dry powder to swollen crystal (though still a solid), to thixotropic gel, to sol.

Before applying the equations of Chapter V to obtain potential energy curves it is necessary therefore to consider the mechanism of expansion of the region W_2 in figure 1(b). According to Barshad (2,3,4), in the dry montmorillonite (vermiculite or other expanding clay mineral) several platelets are sandwiched together with interlayer ions present in the cavities of the oxygen framework which

forms the boundary of the platelets. It is known that the presence of the interlayer ions is essential to swelling, and that this process is dependent on the size and charge of the ion. An important role is also played by the dielectric constant of the solvent medium. In the crystalline region of swelling a few essential things seem to occur. Firstly the solvent molecules, say water, must be adsorbed to the external surface of the crystal; thereafter water molecules penetrate the platelets with concomittant removal of the ions from the cavities of the platelets and subsequent coordination of the water molecules by the ions.

In terms of solid state physics the foregoing process may be considered as the creation of negative holes in the montmorillonite crystal by removal of the ions from the cavities. The interlayer ion now functions as a nucleus for coordination of water molecules to give a heterogeneous crystal of montmorillonite-water. The creation of holes in the montmorillonite and the movement apart of the platelets require energy which must be yielded to the montmorillonite. On the other hand the incorporation of water into the crystal requires that the water molecules release energy. The processes are therefore seen to be complementary, the ions being the main intermediary agents;

extracting energy from the water molecules to be yielded to the montmorillonite and to contribute to the swelling potential. All this may be stated more concisely as, swelling or crystal growth is a consequence of a defect or imperfection in the montmorillonite crystal. The foregoing describes essentially the process in the region of platelet separation $0<2D<5.4\text{Å}$, corresponding to two complete and continuous monomolecular layers of water between any two platelets. It must be borne in mind that the electrostatic models developed are not strictly valid for $2D<5\text{Å}$.

In order to relate the energy extracted from the water molecules, to the hydration energy of the ion, it is necessary to consider the following equation of Bernal and Fowler (6) for the hydration energy of an ion of valence z and radius r

$$U_w = \frac{K_w - 1}{2K_w R_z} z^2 e^2 + (n P_{(r,z)} - u_w) \qquad \text{VI-(1)}$$

where the symbols have the same meanings as in (6). The first term in the above equation arises quite logically from the general electric field equations, while the second term is an empirical relation representing the potential energy change of the water molecules due to coordination by an ion. The term due to the electric field equations has

already been computed in the general expression for U_g. It corresponds to a change in self energy of the ion between vacuum and water which does not interest us since it is stationary with respect to coordinates. In addition the diameter $2R_s$ of the saturation sphere takes values such that it coincides with 2D. This would make the first term zero since the platelet separation 2D corresponds to the upper bound or the physical infinity. From (6, Table VII) $2R_s$=5.8, 7.2 and 9.2 Å for s=1,2 and 3 respectively, which would make the first term negligible. Herein could lie a partial explanation for the lower heats of solution of ions when bound to montmorillonite reported by Jenert (17). It must also be borne in mind that some of the energy abstracted from the polar solvent is yielded to the montmorillonite crystal. Jordan(19) for example, showed that even after separations of 12Å, had been attained, it was still necessary to add polar solvent to commercial montmorillonite-organic complexes in order to obtain further expansion and gelation. This would suggest an energy requirement of the montmorillonite before extensive separation can occur. As shown by Barshad (3) the dielectric constant of the solvent plays a key role. Other factors such as size and type of interlayer ions and solvent molecules are also important as shown by Granquist and McAtee (16). Whatever the interlayer ion may be it

does appear that the solvent should have a high dielectric constant and ability to solvate the interlayer ion thus releasing energy as discussed in the foregoing.

There is no rigorous way of representing the mutual potential energy of coordination of the water molecules by the ion. If as a guide we proceed empirically noting that X-ray studies on montmorillonite and vermiculite in (2,4) and (26,27) show that there is a progressive entry of water (or other solvent) molecules in integral numbers between the platelets. Thus, assuming that the water molecules require a progressive clearance of the order of 2D>2Å, we may devise a step function which will distribute the coordination energy, as a function of platelet separation 2D.

Intuitively this may be represented by an integral function such that

$$(nP-u_w) = (nP_{(r,s)}-u_w)\int_0^{\infty} f(\rho)\, d\rho \qquad \text{VI-(2)}$$

Clearly $f(\rho)=e^{-\rho}$. Proceeding in this empirical manner the contribution to the total potential energy of the system at any interplatelet separation 2D>2Å is now defined as

$$U_C = (nP_{(r,z)} - u_w) \frac{\int_{D-1}^{D} f(\rho) d\rho}{\int_{0}^{\infty} f(\rho) d\rho} \qquad \text{VI-(3)}$$

$$= (nP_{(r,z)} - u_w) \int_{D-1}^{D} e^{-\rho} d\rho$$

$$U_C = (nP_{(r,z)} - u_w)(e-1)e^{-D} \qquad \text{VI-(4)}$$

where D>1.

The interpretation of VI-(3) and VI-(4) is that the fraction of the energy under the curve between $(\rho-1)$ and ρ contributes to the potential energy at $\rho=D$. In a way the function beers some similarity to a Dirac δ-function.

There should also be a term similar to $(nP_{(r,z)} - u_w)$ for the energy yielded to the montmorillonite platelets in order to remove the ion out of the cavity. This term could be developed empirically as above for U_C but the sign should be negative since it is a contribution to U_w. An attempt is being made to estimate this term theoretically. A possibility exists however for estimating its value experimentally. If, for example, montmorillonite flakes of varying ratios of high to low hydration energy ions such as K^+; Na^+K^+; Li^+Cs^+; Li^+ are prepared and then allowed to swell there may exist a critical ratio of ions at which the interplatelet separation takes a value $>9\text{Å}$.*

*See table 1

In this way the critical average hydration energy per ion could be obtained and related to the crystal energy term. This term should to all appearances be much less than $(nP_{(r,s)}-u_w)$ for most ions possessing large hydration energies. Justification for the existence of this term is apparent from Barshad's (5) thermodynamic data for ΔF_w and ΔF_H. Actually from the variation in ΔF_H for various ions of the same valency, it would appear (5) that this term is quite small, decreasing in absolute value as U_C for the ions increase.

But for this negligible unknown term, we are now in a position to compute the total potential energy of interaction in the range ($0<2D<20\text{Å}$) which encloses the so-called (26) crystalline range of swelling for montmorillonite. In this region we are dealing with essentially a solid heterogeneous crystal.

When the interlayer spacings as determined by X-ray studies for plate-shaped macromolecules such as montmorillonite or vermiculite is such that $2D<9\text{Å}$ for all ions, the system is coagulated or forms a unipolar coacervate. Furthermore it is a solid. In order to disperse the system the interlayer spacings have to be increased considerably. This increase in spacing is termed macroscopic swelling (26), since the increase in volume is several fold and somewhat explosive. This type of

behaviour constitute stability phenomena which we also wish to investigate. From Norrish (26) and Norrish and Rausell-Colom (27) the progressive interlayer spacings for montmorillonite, pyrophyllite and vermiculite with various counter ions are reproduced in table 1.

The basis of the theory proposed so far to explain swelling or crystal growth in the crystalline region is amply justified by these data. Pyrophyllite with no defect or imperfection does not swell, since there are no interlayer ions to act as trigger mechanisms. Even in experiments with electric fields to be described, the author was unable to stimulate the pyrophyllite crystal to swell as vermiculite did.

Consider now the mechanism of the explosive process known as macroscopic swelling. It has its basis, the form of the total potential energy and the terms contributing. Figure 2 shows the general behaviour of the energy. In the initial range we have a repulsion arising from ion-solvent and ion-image energy terms, namely equations VI-(4) and V-(6), being predominant. At the intermediate range the surface-ion and surface image terms equations V-(13) and V-(14) which are attractive predominate after contributing to the minimum. This minimum defines the crystalline region and usually occurs around 20-9Å.

Table 1. Maximum Swelling in Different Regions for some Lamellar Crystals

Counter ion	Mineral	Montmorillonite		Vermiculite		Pyrophyllite	
	$-\sigma$ e.s.u/cm^{-2}	3×10^{14}		6×10^{14}		0	
		Crystalline 2D(Å)	Macroscopic 2D(Å)	Crystalline 2D(Å)	Macroscopic 2D(Å)	Crystalline 2D(Å)	Macroscopic 2D(Å)
H_3O^+		0-12	12-30 30-120 ?*	?	?	no interlayer counter ion	no interlayer counter ion, no surface charge
Li^+		0-12	12-30 30-120 ?*	0-5	5-72 72-240 ?		
Na^+		0-9	9-30 30-120 ?*	0-4.3	none		
K^+		0-5	none	none	none		
Ca^+		none	none	none	none		
Ba^{++}		0-9	none	0-5.4	none		
Ca^{++}		0-9	none	0-5.4	none		
Mg^{++}		0-9	none	0-4.6	none		
Al^{+++}		0-9	none	0-4.0	none		

?* Not equilibrium position, constrained by artificial mechanical barriers. For these ions the passage to 2D = 30Å from 12 and 9Å is abrupt with no gradual increase as for spacings 2D>30Å (in the case of montmorillonite). For vermiculite the abrupt expansion is from 5Å to 72Å.

see table 1, and Chapter VII, figures 7,8 and 9. Beyond this range the surface-surface terms which seem to decrease linearly with D and are repulsive dominate, leading first to a maximum and then a path of decreasing energy or a repulsive force (see figures 10 and 11). It is this latter region, that is known as the macroscopic region of swelling. To get over the maximum or to get out of the energy well in the crystalline region, it would appear that U_c must be large enough to reduce the binding energy of the minimum in figure 2 to the order of kT, that is within the range of the ordinary thermal energy at room temperature. If this is accomplished, the ions will become perturbed from their equilibrium positions, generating a more unstable system which can escape over the barrier. Clearly this is a statistical problem which involves a distribution function for the number of platelets which escape the barrier to demonstrate macroscopic swelling. This is borne out by X-ray data of Norrish (26, figure 2) and Norrish and Rausell-Colom (27, figure 3). Naturally the expansion of the first few platelets will act as a trigger mechanism for others leading to an explosive avalanching process.

This may be looked upon from a more experimental view point, to show that macroscopic swelling may actually be artificially stimulated in some cases.

The work of Norrish and Rausell-Colom (27) and Weiss(34 have shown that within certain limits, macroscopic swelling for a variety of clay minerals with various interlayer ions i greater and more explosive the greater the surface charge density. In the second instance the author, by perturbing the mobile interlayer ions of Li-vermiculite with an electric field of afew volts/cm., stimulated Li-vermiculite to exhibit macroscopic swelling almost instantaneously.* These crystals thereafter exhibited similar unexplained electrical properties to those described by Garret and Walker (13). Before giving an explanation to the electrical phenomena in (13) it is of interest to describe briefly the procedure for preparing what seems to be Li-vermiculite. By applying much higher voltages for short intervals to a native Na-vermiculite crystal immersed in water, the crystal was stimulated to swell some three to four times its volume within a few minutes. The water was then replaced by dilute LiCl solution and the perturbation field

*Ordinarily the crystal takes some time before it begins if it is not stimulated artificially.

maintained for a few more minutes. The crystal was then left overnight in LiCl solution, a procedure which is perhaps not essential. The swollen Na-vermiculite when left for a few hours in air always contracted to one and a half times its original thickness. It would appear therefore that the laborious method of prolonged heat treatment used by many workers in preparing Li-vermiculite can be reduced if not avoided. The heat serves largely to increase the ionic conductivity as it would for any ionic crystal lattice.

The explanation for all these electrical phenomena seems to lie in a model presented in (20), that is, consider the vermiculite platelets with the interlayer ions as a pile of plate-shaped conductors. If now an electric field is applied the mobile interlayer ions or positive charge carriers migrate in the direction of the field and can thus be replaced by other positive charge carriers. This perturbation destroys the equilibrium distribution of the ions over the surfaces hence towards the anode there is no shielding between the surface charge of adjacent platelets leading to repulsion and growth of the crystal. The possibility of a permanent dipole moment may be ruled out since there is no preferential direction in the plane for crystal growth, it follows the field completely.

By applying a-c fields of sufficiently low

frequency, the mechanical response time of the crystal could be determined. Preliminary measurements now being perfected would indicate a value of 0.06 seconds. The relaxation time on the other hand depends on the degree of dislocation.

To sum up the surface-surface terms which are linear in D must break down due to edge effects as discussedinn the previous two chapters. When this happens there is the possibility of a second minimum or a singular point as the curves in figures 10 and 11 should approach zero as D increases. We cannot then at this stage define our cut off planes L, or decide whether a second minimmum exists.* From figures 4,5,6,7, 10 and 11 it would appear that the maximum occurs at about $2D=20\text{Å}$ for the monovalent ions with montmorillonite. We therefore have aregion of extreme instability for $10\text{Å} < 2D < 30\text{Å}$, call this the saddle of the potential energy curves. This is just what experiment confirms (26) or table 1. Similarly for Li-vermiculite (27) there is a region of instability given by $5\text{Å} < 2D < 72\text{Å}$. (Seetable 1 again). Clearly the greater range is due to the larger repulsive force or steeper slope to the right of the maxima in figure 11 compared with figure 10. This is to be expected since

*Whe shall not be able to do so until the next chapter. Pertinent to this is the recent work of M. Arnold "The effect of attractive surface ion forces on the permeability of bentonite" Inter. Soc. of Soil Mech. & Found. Engin. 6th. Conf., Montreal 1965 (To be read) which has confirmed figure 2.

for vermiculite is twice as large as montmorillonite. Moreover the larger area of the vermiculite crystals make the surface-surface repulsive force which depends on the square of σ, even more effective, since edge effects are less important.

After the potential energy curves have been presented fully in Chapter VII we shall explore the important question of edge effects more fully. In line with this is the fact that the platelets of montmorillonite are perhaps reasonable flexible (20). It is clear that our models though generally sound will have to take these factors into account.

2. Dielectric Saturation

As discussed in an earlier (20) work, the static dielectric constant of water is hardly suitable in these calculations, since as Debye (10) has shown K_w is a function of distance from the ion. It has already been shown that the general features of the energy are as in figure 2 if K_w is constant.

In Chapter VII it will be seen that when K_w is a function of x these features do not change.

Using Debye's (10) values, an effective piecewise constant $K_w(z)$ was estimated. This was done simply by taking Debye's (10) values stepwise from the ion, as for example $K_w'(1)$, $K_w'(2)$, $K_w'(3)$ ..... $(K_w'(z)$, averaging them arithmetically over z to give $K_w(z)$.

On noting that according to the derivation in (10), $K_w'(z)$ for a single charged or monovalent ion at distance z from the ion is just $K_w'(z)$ for double and triple charged ions at distances $\sqrt{2}z$ and $\sqrt{3}z$ respectively, the values presented in table 2 for ions of charge $e^{\pm}=e$, 2e and 3e respectively were obtained. These and other values for $z>10\mathring{A}$ will be used in the computations.

Table 2. Dielectric Constant of Water after Correction for Saturation

$z(\mathring{A})$	1	2	3	4	5	6	7	8	9	1
$K_w^e(z)$	3.00	3.30	4.50	6.40	9.80	13.9	18.40	22.80	26.90	3(
$K_w^{2e}(z)$	3.00	3.00	3.30	4.25	5.40	7.33	10.14	13.25	16.67	2(
$K_w^{3e}(z)$	3.00	3.00	3.00	3.50	4.20	5.17	6.43	8.25	10.66	1]

It may be noted that as the charge increases, the trend of $K_w(z)$ is such as to increase the absolute value of the electrostatic energy.

Footnotes

The author is fully aware of the limitations implicit in the dielectric saturation theory; but as will be seen it does not affect the general behaviour of the potential energy curves. The values of $K_w(s)$ do in fact approach the static value for large z. Fractions such as α are very insensitive to changes in K_w over a wide range.

The referees of a paper "The Role of Electrostatic Energy Barriers in the Expansion of Lamellar Crystals." J. Chem. Phys. (In Press.) have pointed out that the value of K_w at complete saturation is about 6. In as much as $K_M \simeq 2$, this if anything might improve the agreement between theory and experiment. We hope to take up this suggestion; see appendix.

CHAPTER VII

POTENTIAL ENERGY CURVES

1. Computation and General Remarks on the Stable Location of the charge e*

The computation of the integrals and sums in the equations for U_E was done on the University of Adelaide IBM 620 computer. In order to take into account the effect of electrical saturation the dielectric constant K_W was averaged over the spacing of the platelets according to the formula

$$(K_W)_{av} = (dK_W(d) + (2D-d)K_W(2D-d))/2D \qquad \text{VII-(1)}$$

where $K_W(z)$ is an average value of K_W over a distance z from the ion, obtained from Debye's calculations (10) in a manner described in the previous chapter. In order to simplify computation this same value of $(K_W)_{av}$ is used throughout, the regions occupied by water, although strictly speaking, in model II a constant value of K_W independent of ion situation should be used in regions W_1 and W_3. This gives only a small correction to the location of the points of stable and unstable equilibrium. In Chapter V, section 3, the correct expressions for the electrostatic energy were given for K_W = constant in W_1, W_3.

Some values of $K_w(z)$ have already been given in table I for the cases of single, double, and triple charged ions.

In the first instance we choose for montmorillonite $e=4.8\times10^{-10}$ e.s.u., $A=80\text{Å}^2$, $K_w=2.0$*, $\sigma=-3\times10^{4}$ e.s.u./cm^2, $b=10\text{Å}$, and calculate the energy integrals and sums for 2D in the range $5\text{Å}<2D<20\text{Å}$. From the values of the constants just given we find the following values for the combinations appearing in V-(21) and V-(22):

$$C_1 = e^2/4\text{Å} = 0.575\times10^{-11} \text{ ergs},$$
$$C_2 = 2\pi\sigma e\mathfrak{R} = -0.456\times10^{-11} \text{ ergs},$$
$$C_3 = -2\pi\sigma^2 A\times\text{Å}/K_w = -0.565\times10^{-14} \text{ ergs}. \quad \text{VII-(1)}$$

The constants listed in expression VII-(1) are given for the case of a singly charged ion. For doubly and triply charged ions we replace e by 2e and 3e respectively and R by $\sqrt{2}R$ and $\sqrt{3}R$ respectively.

---

* Naddih (25) gives K_w at 2×10^{4} c.p.s. as 1.62, Deeg and Huber (11) at 3.33×10^{8} c.p.s. as 2.5. Both these values confirm the estimate of $K_w=2$ originally made by the author (21) from the data of Smith-Rose (29,30) on soils. Actually the experiments on dielectric properties carried out in (25), was suggested by the author (20). Preliminary studies on Al and H-montmorillonite were carried out in Professor C. T. O'Konskis' laboratory at Berkely at the author's request as early as 1961.

Some care is required for the computation of the integrals because the integrands all have singularities at the lower end of the range. For the ion-image energy, this singularity can be removed by the change of variable $U=x^{\beta}$, whilst for the ion-surface charge energy, the singularity, which is only present for $\alpha=1$ and depends logarithmically on $(1-\alpha)$, is extracted and the remaining integrals calculated numerically. The singularity at $\alpha=1$ corresponds to the water between the platelets being replaced by a perfect conductor. When these changes have been made, it is possible to compute any integral, for a fixed pair of values of d and D, reasonably quickly.

The first computations carried out on model I with fixed D and varying d showed that the central position of the ion, with $d=D(\beta=\frac{1}{2})$ is energetically favoured. This is not surprising because the symmetry of all these models leads one to expect that the central position will be either one of maximum or minimum energy, and for small d, the repulsive ion-ion forces and ion-image forces will predominate. (It can be seen that $\beta=0$ is a singularity of equations V-(21) and V-(22)). Hence $d=0$ cannot be stable, and must have higher energy than $d=D$. So the central position must be stable. The curves shown in figure 3 confirm this.*

*Actually a plot of the potential in region W for model I gives as a function of z a set of parabolas if we exclude the potential due to the charge. The lowest apex corresponding to $\beta=\frac{1}{2}$.

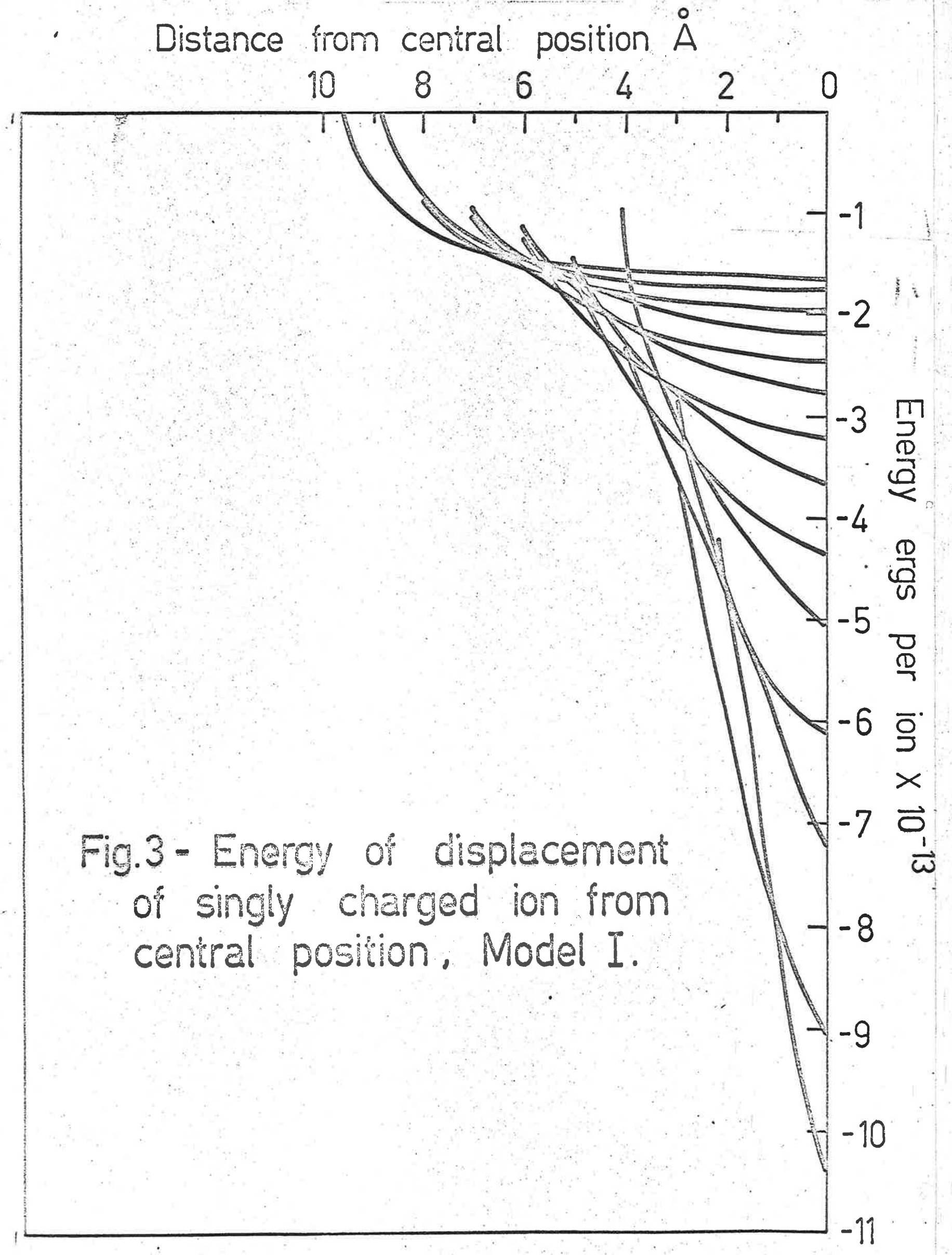

Fig.3 - Energy of displacement of singly charged ion from central position, Model I.

Fig. 4 Electrostatic Energy of Interaction for Model I

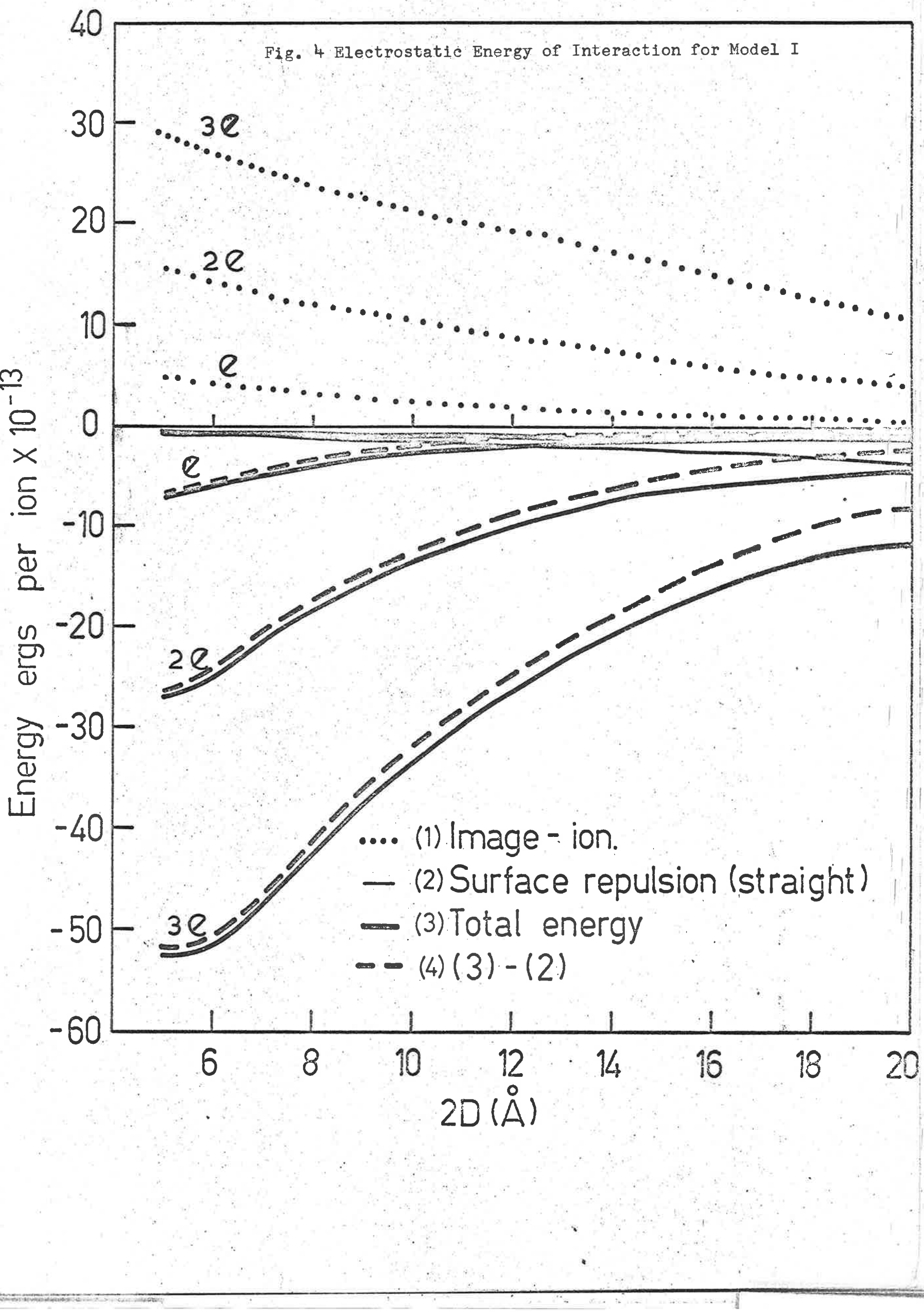

Fig. 5 Electrostatic Energy of Interaction for Model II(a)

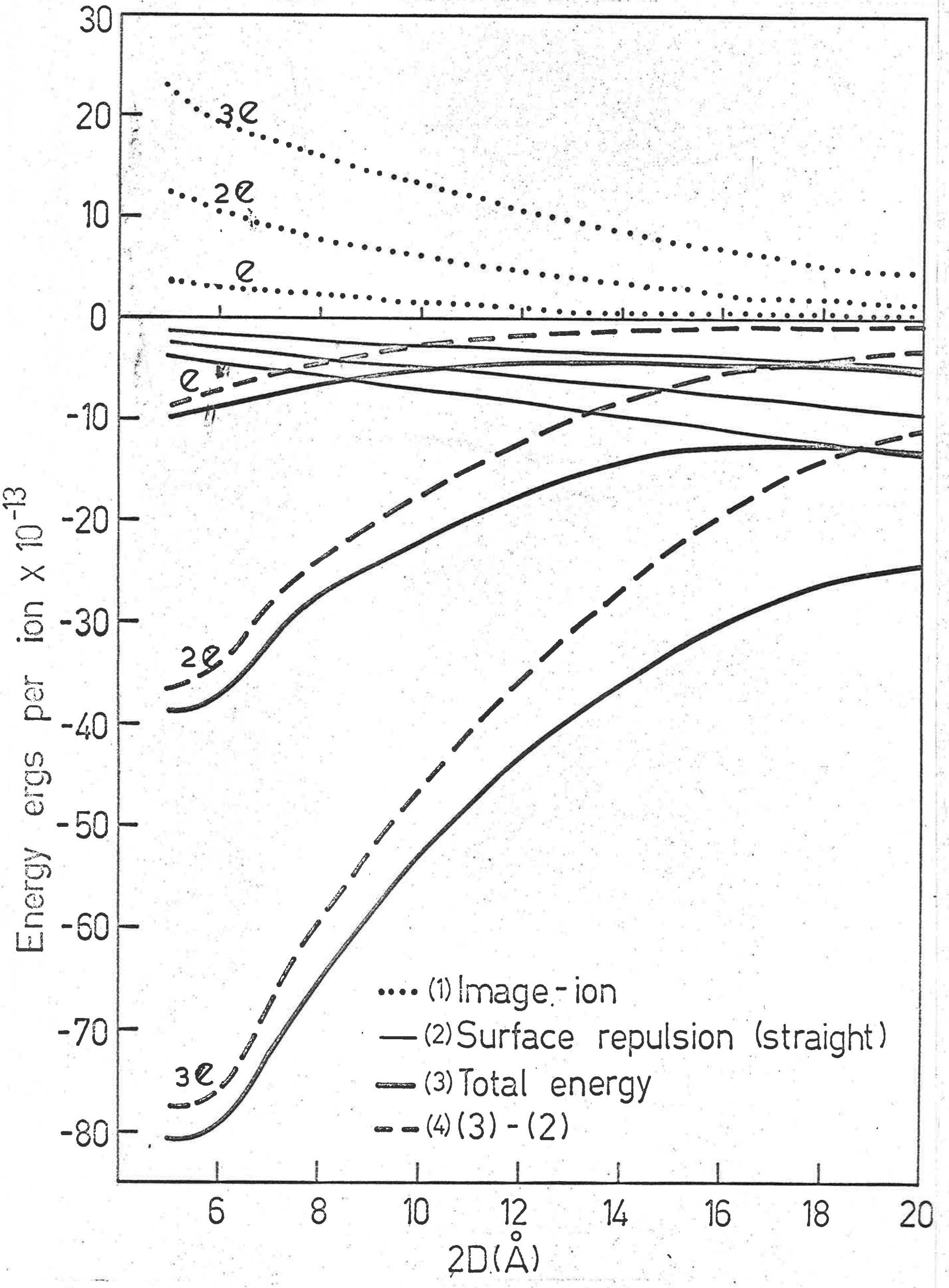

Fig. 6 Electrostatic Energy of Interaction for Model II(b)

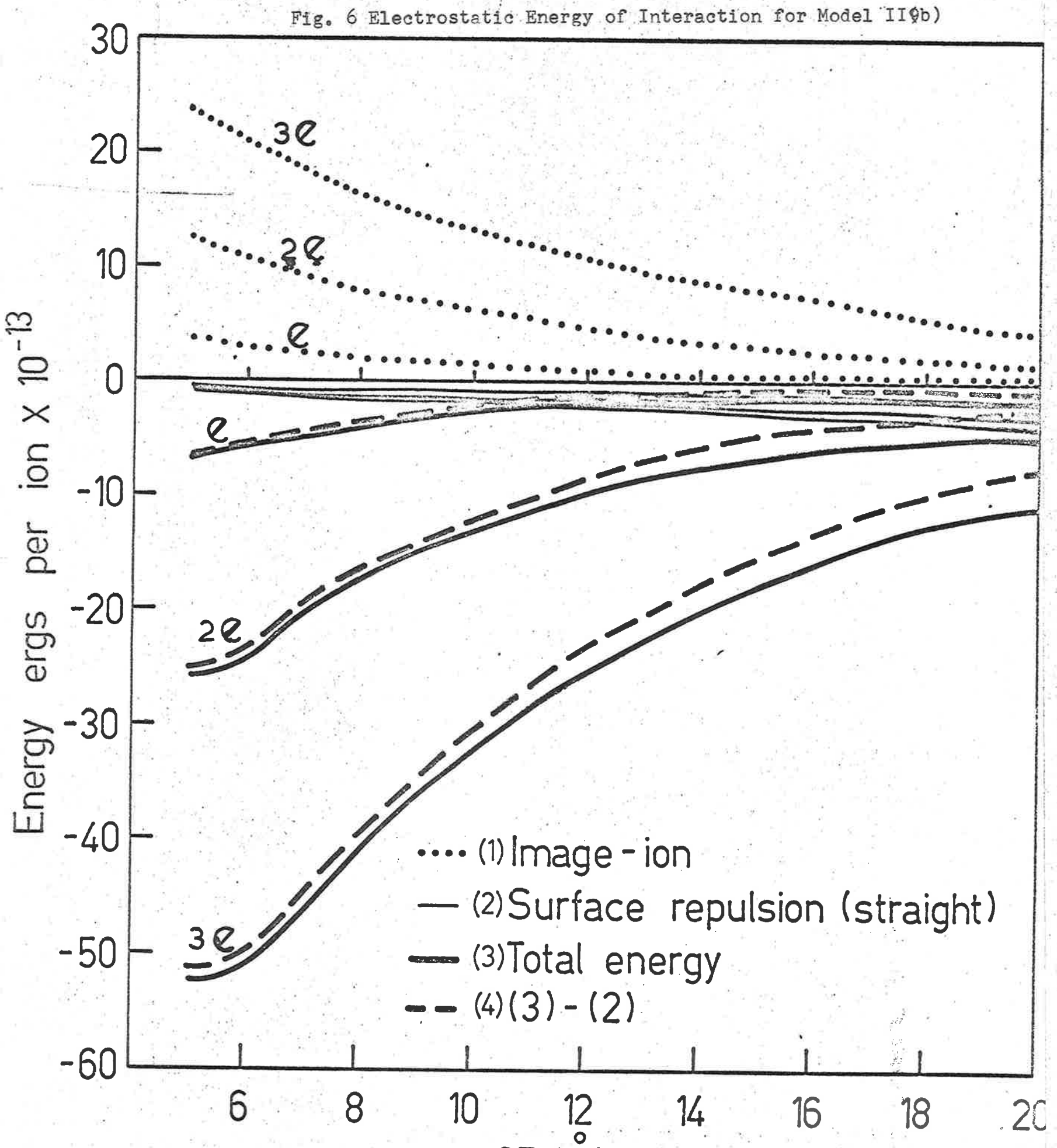

Having established this, it is possible to put $\delta=\frac{1}{2}$ in equations V-(21) and V-(22) and then compute the potential energy curves for the various models based on Fourier and image methods.

2. Electrostatic Energy of Interaction

Below are the curves of equations V-(21) and V-(22) for models I, II(a) and II(b) depicted as figures 4, 5 and 6. As far as possible the significant terms in each equation have been computed separately. Accurate computations of equation V-(2) to be given later in figure 10 show that the curves are identical to those in figure 4 for model I. We may note that there is little to choose between model I and model II(b). Most of the curves also show as expected the possibility of a minimum in U_E as $D\to 2.5\mathring{A}$.

3. Total Potential Energy per Specific Ion

If this is denoted as U_p, it can be estimated but for the unknown crystal-ion term* as

---

* This term can be seen to be a real but small correction term, when the results of theory are compared with Bradhead's thermodynamic data on the swelling of montmorillonite. See for instance ΔF_M in (5, figures 6,7). Compare ΔF_M with $\frac{\partial U_M}{\partial D}$ obtained from the slope of U_M in figures 7,8 and 9. It will be seen that they belong to the same families of curves but for units.

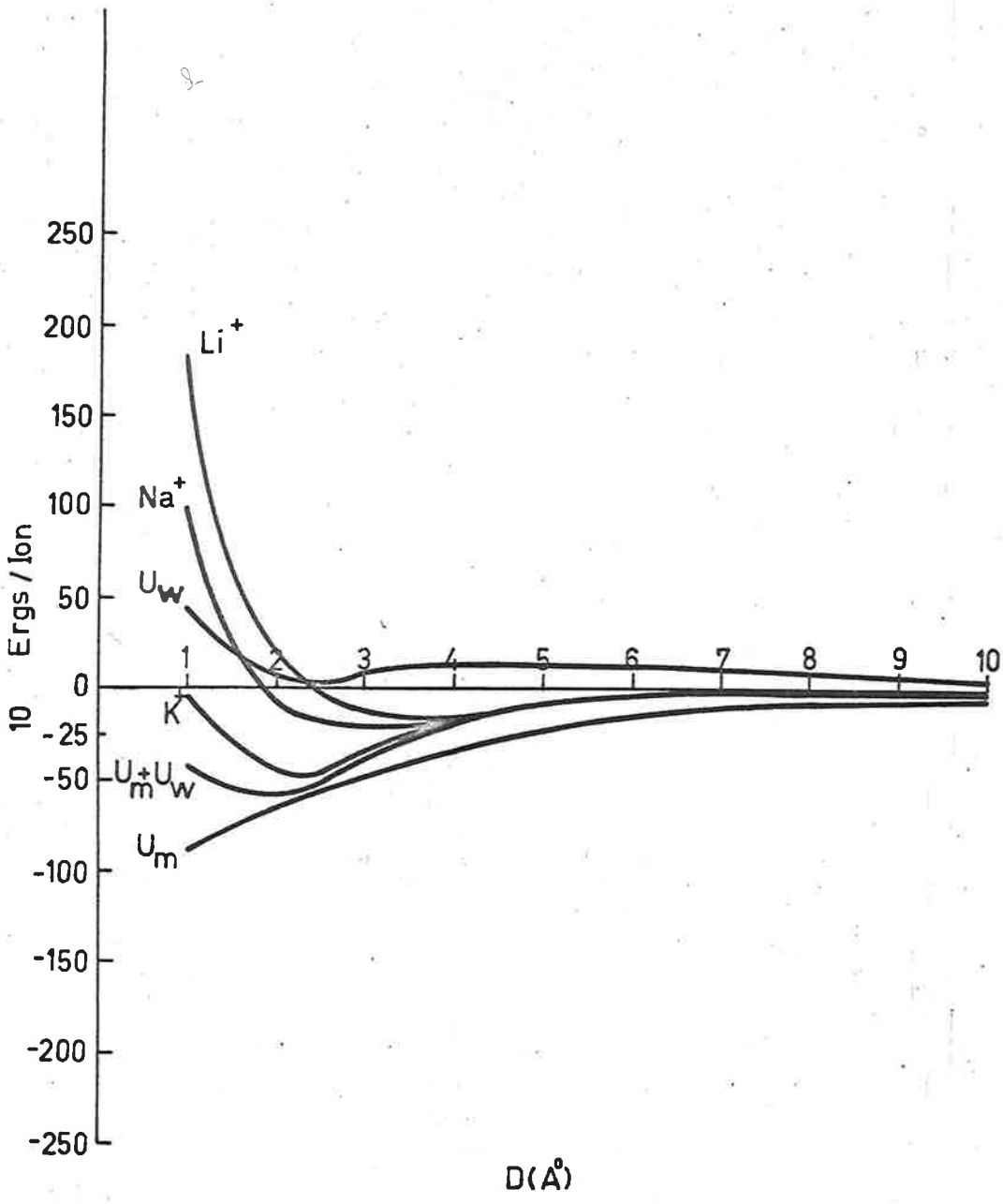

Fig. 7 Energy of Interaction between two Faces of Montmorillonite and Monovalent Ions in relation to half-distance of separation

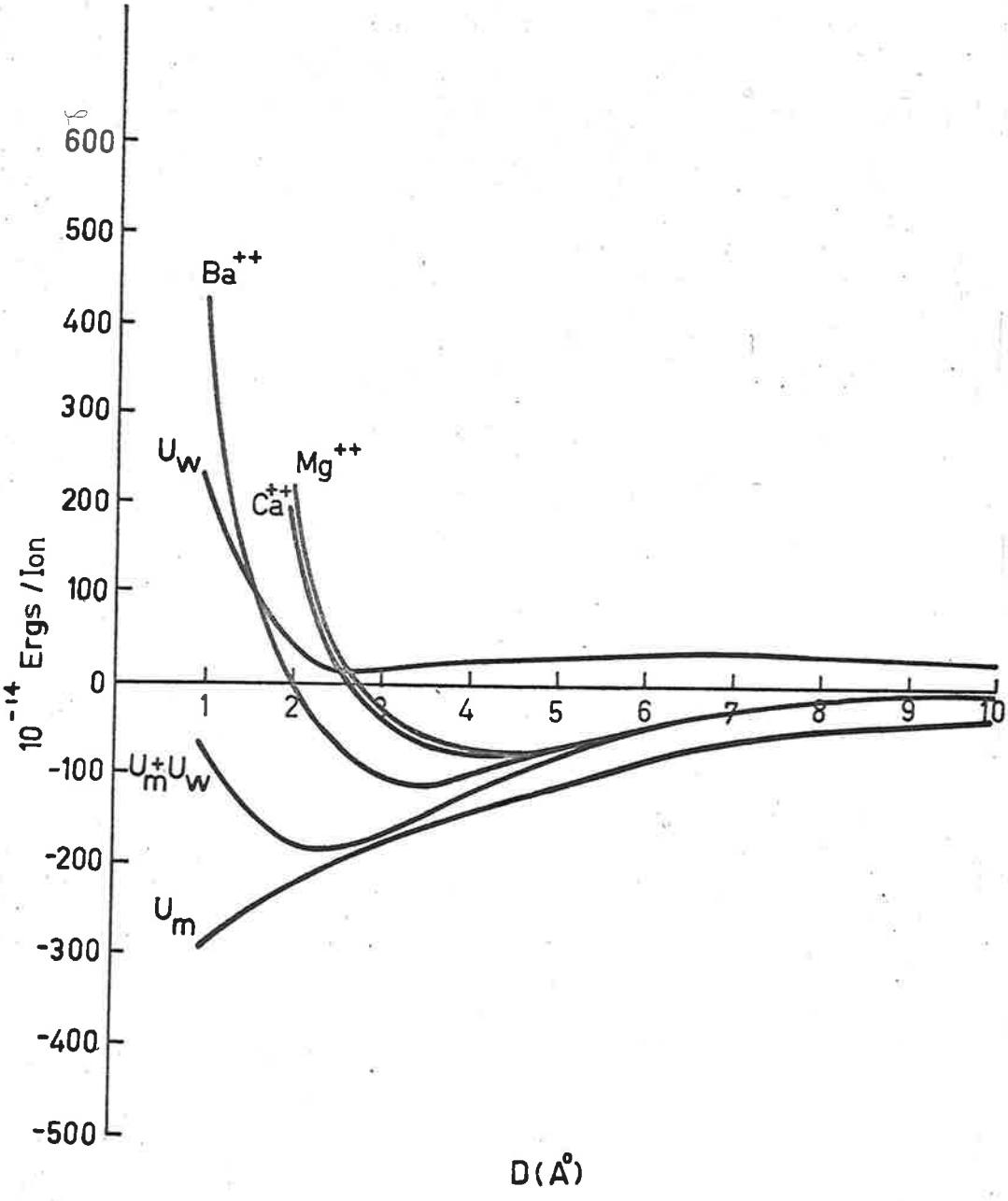

Fig. 8 Energy of Interaction between two Faces of Montmorillonite and Divalent Ions in relation to half-distance of separation

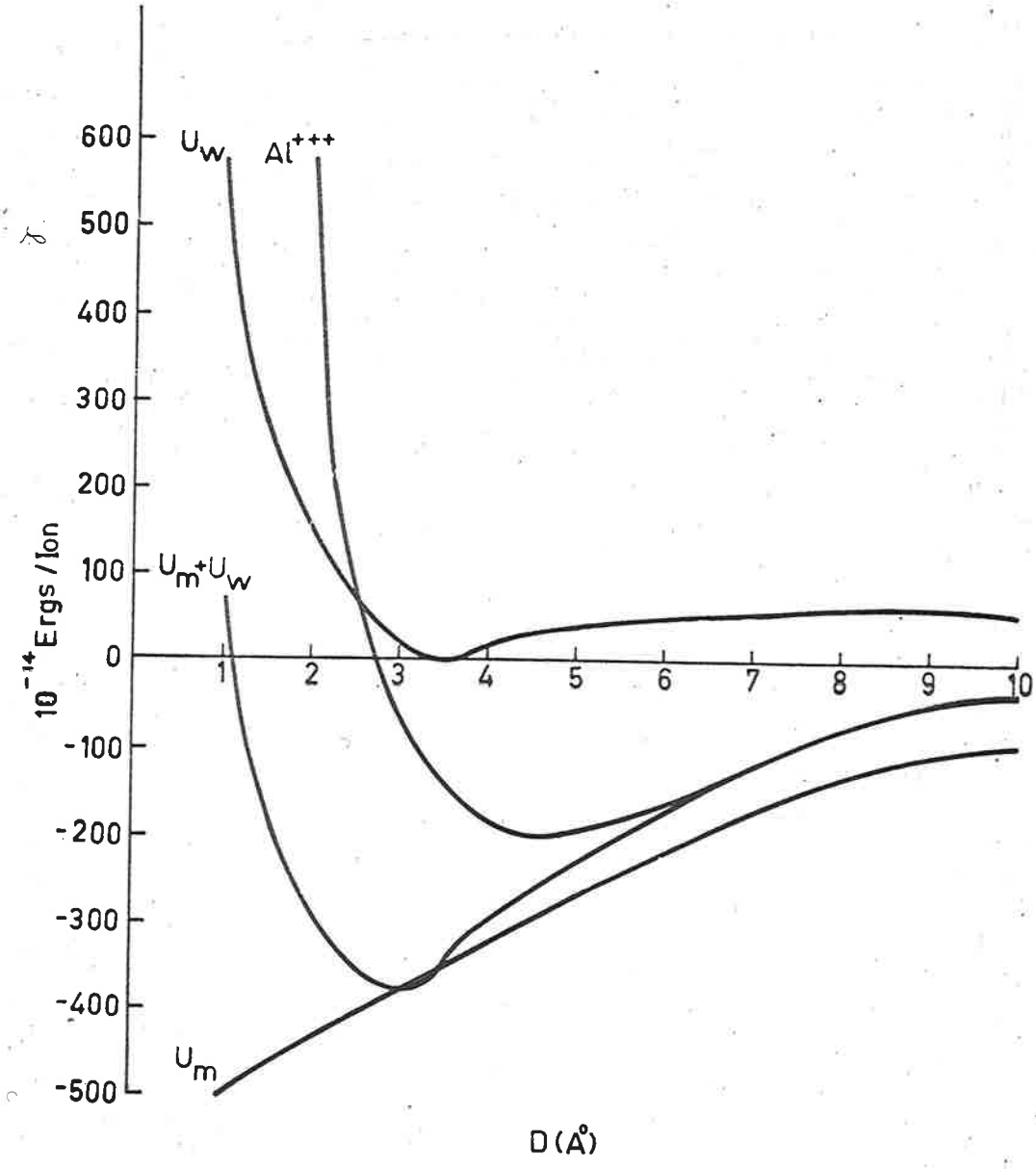

Fig.9 Energy of Interaction between two Faces of Montmorillonite and Trivalent Ions in relation to half-distance of separation

$$U_T = U_E + U_C \qquad \text{VII-(2)}$$

The first computations using V-(2) and VI-(4) in equation VII-(2), yielded the curves shown in figures 7,8 and 9. for ions of various valencies and radii. By superimposing U_C on figures 4 or 6 similar curves can be obtained.

From figures 7, 8 and 9, the estimated position of the minima for the various ions in the crystalline region are 2D~9Å for Al^{+++}, Mg^{++} and Ca^{++}, 2D~7Å for Ba^{++}, 2D~5Å for K^+, 2D~7Å for Na^+ and 2D~6Å for Li^+.

The experimental values are given in table 1. The excellent agreement for polyvalent ions is as was anticipated in Chapter V, whilst that for K^+ shows that the hydration does not have too great an influence in the case of this ion. It can be safely said, that the agreement is overwhelmingly close.

H_3O^+ is omitted because of its well known peculiarities of "ageing" to give a system, which has predominantly Al^{+++} as the counter ion (26,20). If this does not occur however, we can deduce from table 1, that its behaviour would be similar to Li^+ in many respects.

4. Extension of Range of 2D and Edge Effects

The excellent agreement of the position

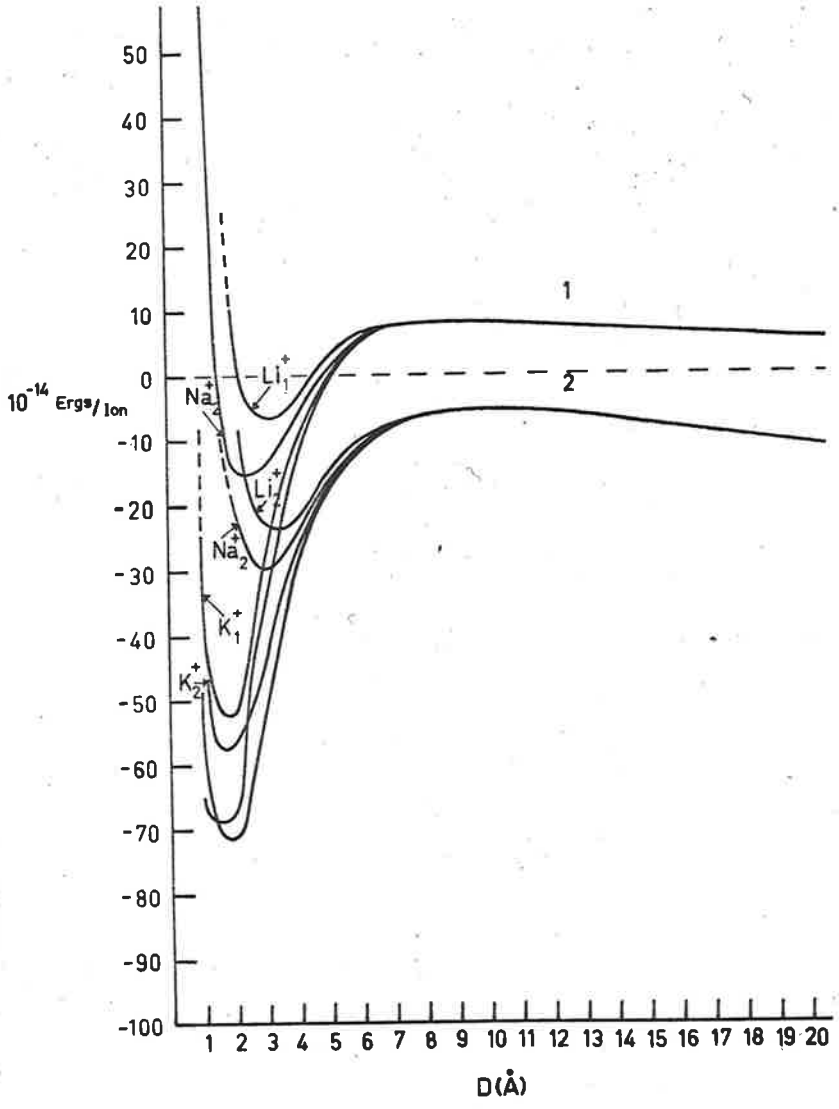

Fig.10(Legend as in FigFig. 7)

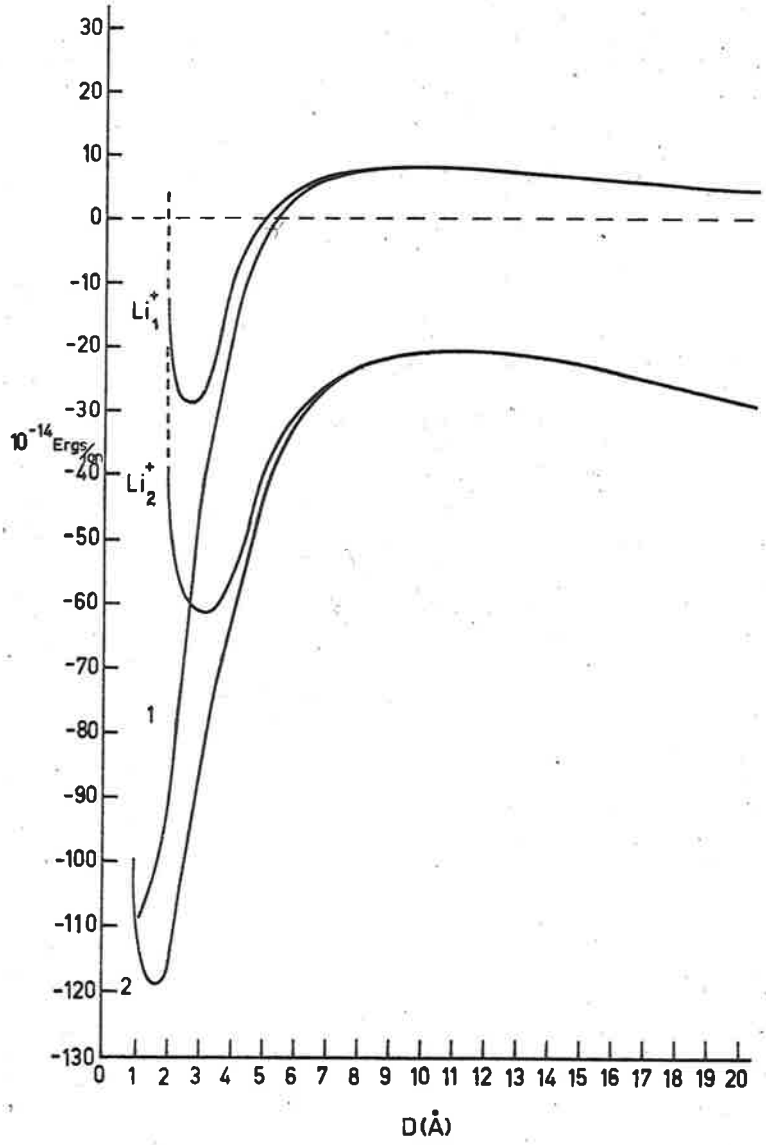

Fig.11 Energy of Interaction between two Faces of Vermiculite and Monovalent Ions in relation to half-distance of separation

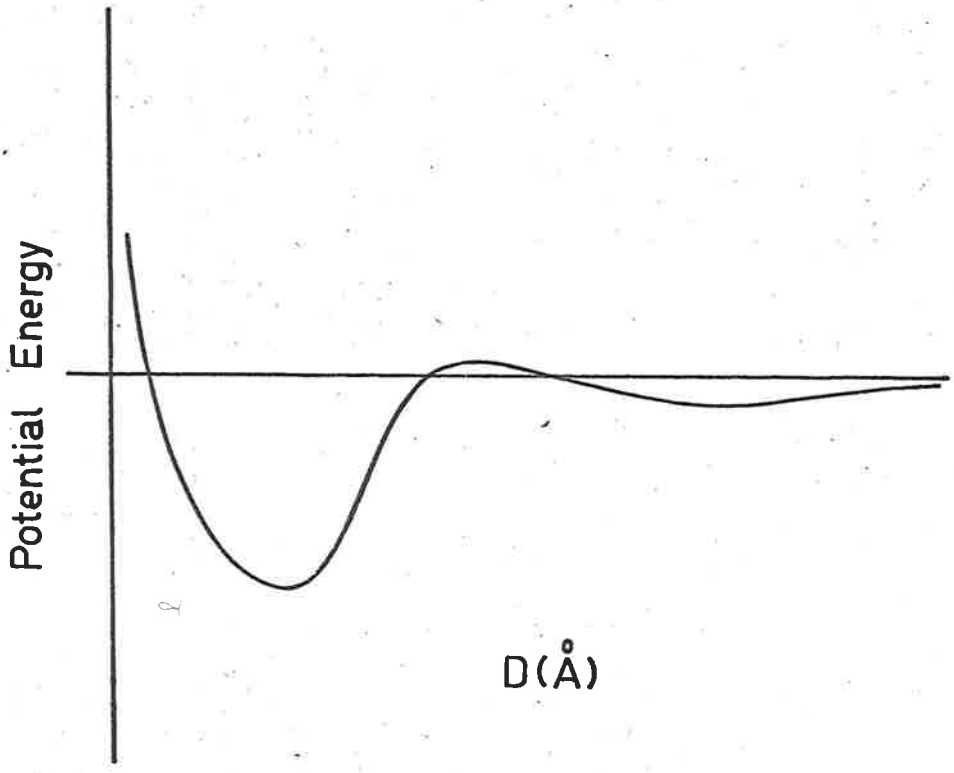

Fig.12 Hypothetical Potential Energy after Norrish(26)

of the minima, suggests that the theory may be valid over a greater range than 5Å < 2D < 20Å.* (Limited to this range in the first instance so as not to clash with classical double layer theory). At least three counter ions are known to exhibit macroscopic swelling outside this range. They are H_3O^+, Li^+ and Na^+ with montmorillonite and Li^+ with vermiculite. Accordingly the computation of equations V-(2) and VI-(4) in VII-(2) is extended in figures 10 and 11. The only change required is an increase of σ by a factor of two for vermiculite, figure 11.

The total potential energy is a compromise between curves 1 and 2 in figures 10 and 11. As the surface-surface terms wane due to edge effects we would expect if U_T is a continuous function of D, curve 2 to approach curve 1 in figure in figures 10 and 11 to yield a single curve like that shown in figure 12.

Perhaps U_T may be only sectionally continuous and there is an abrupt jump from curves to curves in figures 10 and 11.

Consider now for example the charged interface z=0 in figure 1(a), for regions $0 \lesssim z$, instead of a linear

potential in IV-(14), we could propose a bounded non-linear potential which would take care of the edge effects. Such a function is

$$V_\sigma = \frac{4\sigma \sinh h (J_1/2)}{\epsilon_w J_0 J_1^{3/2}} \qquad \text{VII-(3)}$$

where J is a small parameter having units of the reciprocal of length and depends on σ, the area of slabs and other edge factors, such as excess electrolyte, pH, etc.
It is easy to show that VII-(3) reduces to the linear case, that is IV-(14) for x small, as it should. Finally the potential is bounded in absolute value, for as $x \to \infty$

$$V_\sigma \to \frac{2\sigma J}{\epsilon_w J_1^{3/2}} \qquad \text{VII-(4)}$$

which is a finite negative constant. This condition can be made more elegant, by letting V_σ take the value given by VII-(4) as $x \to L$, J being finite. If now we add a constant namely, $-\frac{2\sigma J}{\epsilon_w J_1^{3/2}}$ to V_σ, then V_σ will vanish as demanded in Chapter IV. It is clear that the linear differential equations IV-(1), IV-(2) do not apply. It may be now possible to improve expressions for U_R.

The only change required in U_R is that the surface-surface energy terms which involve the surface

potential V_y explicitly and are linear in D would change to an expression of the general form

$$- \frac{(\sin h\, JD)}{J\, e^{JD}} \text{ ergs cm}^{-2} \qquad \text{VII-(5)}$$

Again for small separations, this clearly reduces to the linear case developed in Chapter V. Thus in the crystalline and near crystalline regions of swelling $2D < 30\text{Å}$, the energy equations of Chapter V are adequate. Before proceeding to extend the range using these equations, we may test their validity against experimental data first.

If now the repulsive force between the sheets of vermiculite at $2D = 30\text{Å}$, is estimated from curve 2, figure 11 by taking slope at $D = 15\text{Å}$. After conversion to dynes per cm^2 with the aid of the factor $-\psi_y/e^o$, a value of the order of 10^7 dynes cm^{-2} is obtained. The experimental data of Norrish and Rausell-Colom (27, figure 6) for Li^+-vermiculite in 0.03 M LiCl yields a force of 4.5×10^6 dyne cm^{-2}. Note that their (27) D' is just $D = 5.5\text{Å}$. It is clear that edge effects and the presence of excess electrolyte are responsible for this reduction in the theoretically possible force. When (27, figure 6) is extrapolated to $2D = 0$, using the majority of the points for $2D > 30\text{Å}$, the

* This would tend to reduce the uniformity of the field due to the surface charge; a well known effect.

intercept is seen to be about 8×10^6 dynes cm^{-2}. (Now 4.5×10^6 dynes cm^{-2} is roughly equivalent to the force of about 4-5 kilograms per square cm. No wonder buildings collapse if this type of force is maintained over a range of distance.)

The force depicted in (27, figure 6) obeys over the region $2D > 30\text{Å}$ an equation of the type

$$F = -\frac{\partial U}{\partial s} = Ae^{-hs} \text{ dynes cm}^{-2} \qquad \text{VII-(6)}$$

where A is a positive constant, (namely the intercept) seen to be approximately 8×10^6 dynes cm^{-2}, and h is a parameter similar to J. We can determine h for different conditions by setting F equal to the residual force observed in (27) and taking the appropriate critical values of $s = 2D$ from (27, table 3). For example, if for pure water the residual force which is a constant (27), be denoted as $F_R = 2 \times 10^4$ dynes cm^{-2} with A taken to be 8×10^6 dynes cm^{-2} and $s = 240\text{Å}$, we obtain for h, the value 0.025Å^{-1}. For 0.03NLiCl, $h = 0.0418\text{Å}^{-1}$. Equation VII-(6) can be quickly checked by computing the force for 0.03NLiCl at any $2D = 100\text{Å}$ and comparing with (27, figure 6). The values are 1.3×10^5 dynes cm^{-2} and 1.4×10^5 dynes cm^{-2} respectively. We can now proceed with some confidence.

Suppose we recognise from figures 10 and 11 that the dominant energy terms for $2D > 20\mathring{A}$ are the surface-surface terms which are linear in D according to Chapter V. If now we replace these terms, by terms such as VII-(5) this will give the type of energy expression to discuss macroscopic swelling. If VII-(6) is integrated with respect to z-(2D) and A is recognised as being proportional to $\pi \frac{m^2}{\beta K_{ij}}$, such a process just yields equation VII-(5) for the potential energy U, if we set b-J. The energy is therefore for $2D > 30\mathring{A}$

$$U = -2A \frac{\sin h\, JD}{Je^{JD}} \text{ ergs cm}^{-2} \qquad \text{VII-(7)}$$

Using (27, table 3) we could now calculate the J-factors. It would then be possible to obtain a family of curves for different LiCl concentrations and also to interpolate for others. We must remember that J also depends on σ and on the area of the vermiculite crystal. A similar but more difficult analysis can be carried out for montmorillonite.

Interesting features about VII-(7) are that it describes a path of decreasing energy, approaching the finite value of $-\frac{A}{J}$ ergs cm^{-2} asymptotically, and hence the repulsive force though of exponential order never vanishes for z finite. The energy has no proper minimum but

infinity is a singular point where the force vanishes and the energy takes a finite constant value. If there were no other forces acting on the system z would go to infinity theoretically. In actual practice surface tension, viscous resistance, gravitational forces and mechanical barriers in the apparatus and system provide counter-balancing forces which perhaps contain the system abruptly and make the physical infinity as distinguished from the mathematical ideal, a finite value of z.*

We can change the reference state of the energy by simply adding the constant $\frac{A}{y}$ to both sides of VII-(7). This will make U vanish at infinity and exhibit a curve resembling curve 1 figure 11. $\frac{A}{y}$ for Li-vermiculite in water is only about 2.56×10^{-14} ergs/ion or roughly $\frac{1}{6}$ kT, and is certainly effectively zero or close enough.

Actually all this might not be necessary because if U_y given by equation V-(18) is used in V-(2), we find that V-(18) and U_y are very delicately balanced energy terms in the macroscopic region. As 2D increases they approach each other ever so closely. At $2D = 100\,\text{Å}$ for example, their difference for a monovalent ion, that is curve 1 in figures 10 and 11 is only about 2×10^{-14} ergs/ion or close to $\frac{A}{y}$ both for montmorillonite and vermiculite.

*Hence there is a residual force N_R

The concept of U_M given by V-(14) opposing U_W V-(18) is very attractive for explaining thixotropy. U_M gives an attractive force while U_W gives a repulsive force of roughly the same order of magnitude. It is well to note that both U_M and U_W can be written in the form of a decaying exponential term, such as the second term in V-(21), hence both are of exponential order. Their resultant force is clearly similar to equation VII-(6) which is based on experiment (27). The effective capacity of this force to do work is cut off as already explained, when it approaches the value $F_R \sim 2 \times 10^{4}$ dynes cm^{-2} for Li-vermiculite at a given distance 2D, depending on J, that is electrolyte concentration and other edge factors. If this critical distance 2D be considered an extremum or a singular point then by perturbing the system with an external force, electrical or mechanical we will disturb the equilibrium. At once, the delicately balanced forces will tend to restore the system, if the perturbing force is removed.

This is exactly what seems to happen when a thixotropic system is perturbed. Since the constitutive forces of the system $-\frac{1}{2}\frac{\partial U_M}{\partial D}$ and $-\frac{1}{2}\frac{\partial U_W}{\partial D}$ are small, the cohesive forces of system can be disrupted, that is, the particles, if small enough, act independently of each other and hence the system

will behave like a fluid instead of a heterogenous crystal. Perhaps this is part of the ultimate explanation to the peculiar electrical phenomena described in Chapter VI and (13).

The author wishes to add however that specific edge effects in the case of montmorillonite are not ruled out. We must also note that in some cases, the gel can be permanently disrupted, since some particles may even return over the maximum to the minimum, while others separate completely.

A very important point in regard to edge effects is the fact that the platelets of montmorillonite for example, are flexible (20). Now due to edge effects, the efficiency of the swelling force will not be uniform over the entire surface of the platelets. It is fair to expect that 2D will vary over the immense areas if these platelets exhibit some flexibility. Different regions of the surface could be in different states of potential energy, figures 4 to 12, some binding some non-binding.

Is it therefore unreasonable to propose that thixotropy and gel strength may be related to this behaviour?*

To quote from the author's first research report on electron-microscopy, 1960 (unpublished):

* Manifested in an interchange of binding and non binding regs of the flexible particles due to external perturbations, giving rise to associated relaxation and thixotropy

"Montmorillonite on the other hand yields such an seemingly intricate picture, that it is exceedingly difficult to say precisely what its shape is in water suspensions. It does seem to consist of thin flakes rather than ordered sheets. These flakes may be like coiled ribbons, folded over on themselves in a variety of ways. One might consider montmorillonite particles in water, as being essentially a set of coiled ribbons, which cross each other to produce miniature plateaus or sheets at intervals. This is probably a reverse description of the system, since the dry montmorillonite particles were probably wholly parallel sheets which developed into ribbons, due to differential adsorption of water molecules by the cations and the clay particles. At low magnifications and poor dispersion (colloid) ribbons are not distinct." The discussion in (20) should also be considered in this context.

To sum up, it is now proposed that instead of the classical linear expression for the potential of plane surfaces with free surface charge found in most texts, we use a non-linear expression* such as

$$V_r = \frac{4\pi\sigma}{J\varepsilon_r}\left[\frac{\sin h\,(Jz/2)}{e^{Jz/2}} - \frac{1}{2}\right] \quad \text{VII-(8)}$$

The J-factors for particular lamellar crystals have to be

*Or some similar approach to consider edge effects since it would appear that edge factors hold the key to a complete understanding of lamellar crystals and plate-shaped colloidal particles.

determined by experiment at the moment. Further advance in theory may show how they are reciprocally related to L, the cut off distance. If so L for Li-vermiculite in pure water would be 40Å.* The choice of a non-linear potential may seem counter to the superposition theorem, but it is quite clear that the theorem was devised with point charges in mind.

We may further conclude, that there is only one minimum in the energy for the Li-vermiculite system and that is shown in figure 11, further curve 1 in figure 11 is perhaps closer to the experimental situation. We may therefore eliminate the second minimum in figure 12. In other words the compromise between curves 1 and 2 is such as to favour equation V-(16) and equation VII-(5) over V-(17). The linear potential for a charged plane interface IV-(14) is only an approximation to VII-(8) and can only be used in the immediate neighbourhood of the interface, that is z small. Beyond this we must have a force like VII-(6) and consequently the electric field of exponential order.

*If so, the repulsive surface-surface terms would dominate the energy from the maximum in figure 11 to 2D = 2L = 80Å. We may recall from table 1 that for Li-vermiculite there is an explosive unstable region from 2D = 5Å to 72Å. Thereafter the crystal swells gradually as if the swelling forces have been damped considerably.

CHAPTER VIII

DISCUSSION AND IMPLICATIONS

1. General Discussion and Implications

From the equations of U_g for the different models and their representations in figures 4 to 11, it is clear that the electrostatic energy of interaction is such a function of distance as to exhibit a minimum or energy well. This minimum arises from the combined effects of dielectric image or polarisation energy terms and coulombic terms. As shown in the previous chapter, the repulsive image terms are not adequate in the crystalline region and the solvent-ion interaction or hydration energy must contribute. The best agreement between theory and experiment is seen to be obtained for polyvalent ions and for monovalent ions of low hydration energy since U_p is determined largely by U_g. For Al^{+++}, Ca^{++} and Mg^{++} there is almost perfect agreement in the position of the minima. This is to be expected since the larger the surface element of specific ion interaction $e^2/2r$, the more ideal the model becomes.*

The depth of the minimum in the total potential energy curve for Al^{+++} in figure 9, suggests that the binding energy is about 30 k.cal. per mole of ions; a value which is about one sixth of that for the sodium chloride crystal.

*Of course there is much room for improvement in estimating the hydration pressure.

Such a correlation indicates why Al-montmorillonite does not exhibit macroscopic swelling. On the other hand Li- and Na-montmorillonites, figure 7, show binding energies of the order of 3 and 4 kT respectively. Such minima are shallow enough (of the order of 3kT) to permit macroscopic swelling as experiment confirms (26). No such luck for K^+.

Since the binding energies of the various ions determine the potential energy and stability of the surfaces, this feature may have general biochemical implications.

In figures 7 and 8 there is a marked difference between the biological important ions such as K^+, Na^+, Mg^{++} and Ca^{++} compared with Li^+ and Ba^{++}. Thus K^+ and Ca^{++} which assist in maintaining the osmotic and structural integrity of living cells have high binding energies and would thus maintain a surface in a state of relatively stable potential energy. Of course at the other extreme is Cs^+ which would virtually immobilise a surface. Ca^{++} has perhaps ideal properties for biological functions in that while it facilitates a good turn-over of water, it also has a high binding energy.

This could explain the well-known regulatory influence of Ca on the uptake of some other ions by excised plant and animal tissues.

Since

$$V_B^* = \frac{\partial U_B}{\partial e^*} \qquad \text{VIII-(1)}$$

it is possible to compute the change in potential in the regions in figure 1(a) and 1(b). It is easy to show there is an increase in V_B^*, if we exchange K^+ on a surface for Na^+. For every 10^{-14} erg/ion decrease in binding energy, we get an increase of about 0.00625 volts. Thus if $\Delta U_B = 20 \times 10^{-14}$ ergs/ion for K^+ to Na^+, the potential rise is 0.125 volts in the region of the surface, with which the ion interacts. This clearly has a bearing on the transfer nerve impulses. While these correlations cannot be taken too far, there does seem to be some relationship between these properties and the total potential energy spectrum displayed by the various ions.

From the curves in figures 7,8 and 9 representing U_M, U_W and U_E, it is seen that U_M is the leading term of U_E in absolute value. This evidence does seem to favour the theory of swelling proposed in Chapter VI that there is an energy requirement of the montmorillonite platelets which must be satisfied by cooperative processes between the solvent medium, the interlayer ion and the platelets before any appreciable expansion can proceed. This is accomplished by U_C and U_{We} and ordinary thermal energy. The hydration energy term may be looked upon as a trigger

mechanism, for what seems to be basically an electrostatic process.

It may be noted again that if the platelets were conductors U_g would be zero. It is interesting to compare the slopes of (U_g+U_c) and U_g in figures 7, 8 and 9, with their equivalent $\Delta\bar{E}_g$ and $\Delta\bar{F}_g$ in Bernhed's thermodynamic data (5). The units in (5) are not obvious but the agreement between the families of curves in (5, figure 2 to 8) and figures 7, 8 and 9 is overwhelmingly in favour of the image theory. Later it may be possible to obtain a more accurate comparison, if the units in (5) can be clarified.

In the figures 4 to 12 the curves of equations for U_g, U_g and U_T all have the typical appearance of potential energy curves for molecular systems. The explosion to a gel by montmorillonite or vermiculite crystals, may be regarded as the probability of skating out of the energy well. There is therefore a statistical problem* or a distribution function for the number of platelets which escape the barrier to demonstrate macroscopic swelling. This is borne out by X-ray data of Norrish (26, figure 2) and Norrish and Rausell-Colom (27, figure 3). It is well to note that expansion of the first few platelets will act as a trigger mechanism for others, leading to an explosive avalanching process.

* Pertinent work is Mitchell J.K. "Shearing Resistance of Soils as a Rate Process" J. Soil Mech. & Found. Div. Proc. A.S.C.E. 90, SM1 29-61 (19 It is interesting that he estimates the binding energy in a clay of mixe ionic composition as 100×10^{-14} ergs/bond. Compare figures 7, 8, 9.

These potential energy curves in this work also have implications for engineers and any materials scientist. Consider for example the well known* anomaly of maximum density and sharp rise in permeability coefficient observed during consolidation of a predominantly Na-clay (montmorillonite) soil by a civil engineer or soil physicist. These studies over the years, have shown the presence of a mystifying latent attractive force, at clay platelet-platelet spacing of about 30 or 20 to 10Å. In terms of figure 10 for example, it is seen that as soon as the platelets are brought to the maximum ~2D=20Å there is a built in attractive force down to the minimum and then a repulsive force as 2D->0. In any effective stress theory in soil mechanics, these forces have to be considered. The attractive force between 2D=20 to 10Å will surely cause the permeability coefficient to increase, by expelling the water. In terms of figures 1(a) and 1(b) there is a tendency for the medium in regions W and W_1 to be expelled until the minimum in U_T is approached. This example involves mainly the so-called crystalline and near crystalline regions of swelling, where the developments of Chapter V are adequate without any reservations. The attractive force as estimated from the potential energy curve for two Na-montmorillonite platelets is about 10-15 $kg.cm^{-2}$ at 2D=19Å. If this force is only 30-50%

* For example 1) McRae T.L & Turnbull W.J. Proc. A.S.C.E. 89, SM6 101-108 (1963).
2) Jennings J & Burland J. Geotechnique XII No 2 125 (1962)
3) Ref in Footnote, p. 87.

efficient, then it would account for the consolidation anomaly *

Finally we may note that since consolidation is essentially the reverse process to swelling, this evidence is strong support for the general form of the potential energy curves obtained by the theory of electrostatic models.

We now consider as another example which involves the macroscopic region, the interesting problem of quick clays and their basis, thixotropy. For this, all we need are the developments of Chapter VII, section 4.

2. Concluding Remarks and Speculations

The Fourier transform method had yielded solutions which are equivalent to those obtained by image methods. The hydration energy of counter ions is shown to act as a trigger mechanism for what seems to be essentially an electrostatic phenomenon. The midway position of the charge is shown to be favoured energetically and the behaviour of the total potential energy curves to be in accord with experiment.

The general theory of electrostatic models has yielded a result which supports Langmuir's (22) preliminary ideas convincingly. All the evidence from theory and

* Also Grim's paradox (R.E. Grim, App. Clay Technology, McGraw-Hill p.250, 1962) of high initial swelling pressures for polyvalent ions, yet no polyvalent ion swells in macroscopic region (table 1) can be readily explained by the initial slope or depth of the minima for the curves in figures 7, 8, 9.

current experimental knowledge suggests that within the limits set by the type and size of solvent and interlayer ion, swelling and many other colloidal properties of clay minerals is wholly determined by the electrical properties of the system. The influence of the surface density of charge on swelling, points to the fact that double layer theory in its present form is not always applicable to clay mineral systems. As further proof of the importance of the dielectric constant of the medium between the platelets a comparison may be made of (3, table 7) and (34, table 1). Here it is seen that a Ca saturated montmorillonite immersed in a mixture of octanol and n-pentane gives almost the same X-ray spacing as a montmorillonite saturated with n-octyl-ammonium ion in a mixture of n-octanol and n-octylamine. This result would indicate that in this range of dielectric constant of the solvent, the alkyl-ammonium ions behave similar to any other ion and support is also given for Barshad's (3) proposal of complex formation between the solvent and the platelets of montmorillonite. Moreover these complexes should be regarded as heterogenous crystals as in Chapter VI and not as liquids.

Finally we may speculate as to other problems. One such is to consider arrays of platelets, with ions regularly placed in the intervening liquid medium as in a

vermiculite or montmorillonite crystal. This problem is faced with algebraic and computational difficulties only.

There is also the question of other geometries. Consider the case of two approximately spherical protein particles B and C in a bipolar coacervate. A simple first order solution would be to consider that B sees C as a point charge and vice versa. At very close approach, the surfaces facing each other could be approximated to semi-infinite planes with point charges at their boundaries. If the distance between B and C is 2D, then since the planes are not infinite, we take only the first images. If the solvent-charge interaction is also taken into account as in Chapter VI, then it is likely that we will get a positive energy term like U_C, an image-charge term like the first in equation V-(23) and finally the well known negative charge-charge or coulombic term. Clearly we have the prospect of a minimum in the energy of interaction at some separation 2D. The need for this minimum has already been outlined by Langmuir (22) and in Chapter I of this work in discussing (22).

This same problem may be approached more rigorously to give inifinite sets of images using this same model, except that the spheres need not be approximated to planes. Chapter II, section 2 and Chapter V, section 3

indicate methods to do this. It is quite doubtful whether the rewards would merit the effort.

CHAPTER IX

APPENDIX

1. Double Layer Theory: Successions and Extensions for Clay Mineral Systems

This problem has already been alluded to in Chapter V, section 3. Before outlining the suggestions it is well to get a clear idea of the process we are considering. Double layer theory is quite preposterous below 2D=30Å since this is a problem of the solid state. The maxima at 2D=20Å in the potential energy curves for Li and Na-montmorillonite, represent the critical points for transition from a solid to a gel. At this stage the heterogenous crystal of montmorillonite-water ruptures. It does not return to pure montmorillonite platelets and free water however. Instead a platelet of montmorillonite-water is obtained. According to (26,27) the effective thickness is now b=21Å, instead of b=10Å given in Chapter VII, section 1. This is a heterogenous material whose dielectric constant is no longer $K_M=2$ as for pure material. Based on (29,30) and earlier discussions with Professor C.T. O'Konski and Dr. Shirai (20) a suitable choice of dielectric constant is $K'_M=20$. This is the high frequency (about 3×10^8 c.p.s.) value for montmorillonite with 20-30% water content (by weight).

We are now in a position to set up a double layer

problem.* It seems reasonable to set $\sigma=0$, on the assumption that the water layers of 5-6Å with the equivalent counter ions imbedded on either side, would make the resultant heterogenous crystal neutral. Actually we may go further and suggest, that it is in an effort to achieve this state of crystalline perfection, that swelling in initiated. Returning to figure 1(b) the model has the following changes: K_g and b become K_g' and $b'=b+11$Å respectively, while in regions W_1, W_2 and W_3 we have a volume density of charge ρ, defined by Boltzmann's theorem. Finally $2D>30$Å. Now the problem is completely set up, all the rest is computation and algebra only.

In as much as Verwey and Overbeek (33) have written a book on a simpler problem, the author will present the solution in another publication. Preliminary results show that the general form of curves 1 in figures 10 and 11 for $2D>30$Å is not altered.

*Instead we might follow F. P. Buff and F. H. Stillinger J. Chem. Ph. 39, 1911 (1963). In figure 1(b) place additional interfaces at $z=-(b+6)$Å, 6Å, $(2D-6)$Å and $(2D+b+6)$Å, where $-(b+6)<z<-b$, $0<z<6$, $2D-6<z<2D$ and $2D+b<z<2D+b+6$ define new dielectric regions of water, compr Saturated electrically. If we now remove the charge at $(0,0,d)$, we con arrays of charges in the planes midway between the new interfac and the old interfaces adjacent. We may further choose to hav a volume density of charge in the remainder of regions W_1, W_2 and or in order to simplify matters regard them as just dielectric regions. The regions of complete saturation may be taken to have a dielectric constant of 6.

To solve this problem would require nine expressio in equation IV-(19) and of course much more algebra

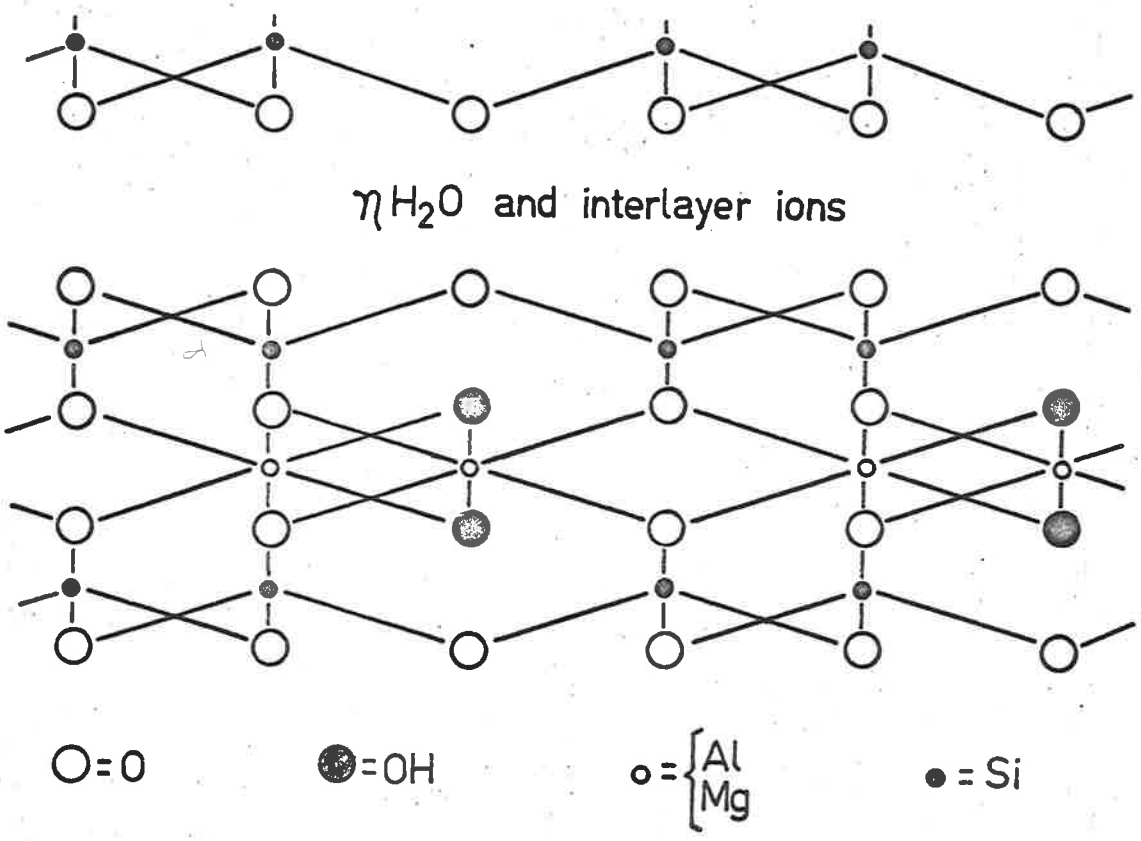

Fig.14 Crystal Structure of Imperfect Pyrophyllite or Montmorillonite (Usually Mg/Al= 0.66 giving roughly one electronic charge per ~~ten~~ 18 peripheral oxygens)

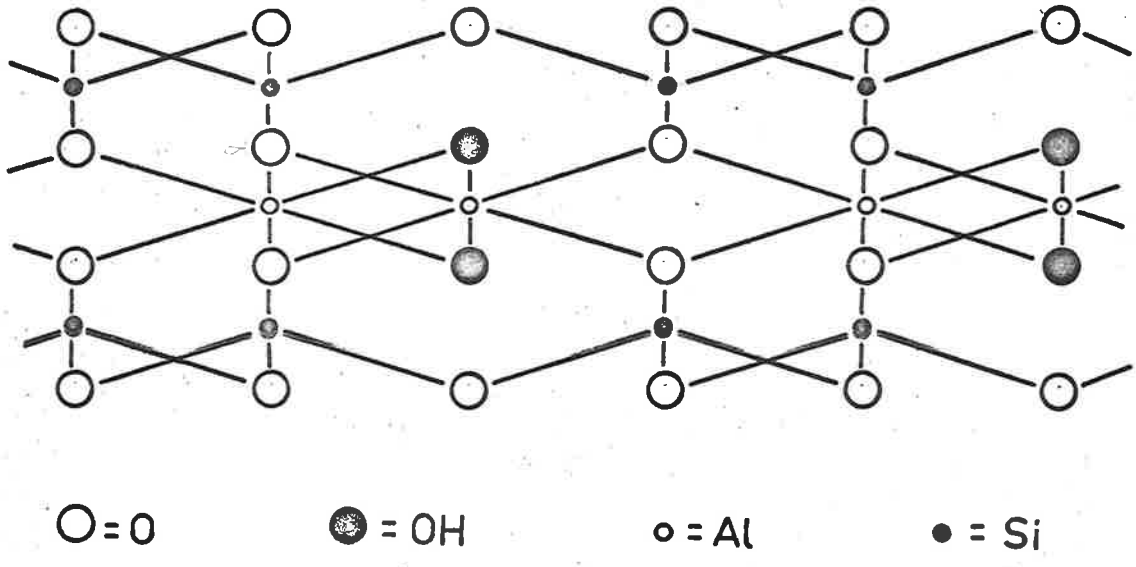

Fig.13 Crystal Structure of Pyrophyllite

CHAPTER X

REFERENCES

1. Barnes, E.W., Quart.Journ.Math., 138, 155 (1903).
2. Barshad, I., Amer.Min., 34, 675 (1949).
3. Barshad, I., Soil Sci.Soc.Amer.Proc. 16, 176 (1952).
4. Barshad, I., Clays and Clay Technology, California Div. of Mines, Bull. 169, 70 (1955).
5. Barshad, I., Clays and Clay Minerals, 8, 84 (1960).
6. Bernal, J.D. and Fowler, R.H., J.Chem.Phys. 1, 515 (1933).
7. Brown, G.A., Mineralog.Soc.Gr.Britain Clay Mineral Bull. 4, 109 (1950); quoted in Grim, R.E., Clay Mineralogy, p. 134. McGraw-Hill Book Co. Inc., New York, Toronto, London (1953).
8. Chapman, D.L., Phil.Mag. 6, 475 (1913).
9. Debye, P. and Huckel, E., Physik Z., 24, 185 (1923) 25, 97 (1924).
10. Debye, P., Polar Molecules, Dover Publications Inc., New York.
11. Deeg, E. and Huber G., Ber.D.K.G., 32, 261 (1955); quoted in Martin, R.T., Clays and Clay Minerals 9, (1962).

12. Derjaguin, B.V., Disc.Faraday Soc. 18, 85 (1954).

13. Garret, B.C. and Walker, G.F., Clays and Clay Minerals. 10, 557 (1963).

14. Gouy, G., J.Physique (4) 9, 457 (1910).

15. Gouy, G., Ann.d.Phys. (9) 7, 129 (1917).

16. Granquist, W.T. and Mattee, J.L., J.Coll.Sci., 18, 409 (1963).

17. Jenert, H., J.Agri.Sci. 24, 136 (1934); quoted in ibid ref. 7, p. 187.

18. Jeans, J., Mathematical Theory of Electricity and Magnetism, 5th ed., Cambridge University Press, Cambridge, England (1960).

19. Jordan, J.W., J.Phys. and Colloid Chem., 53, 194 (1948).

20. Jordine, E.St.A., Bodman, G.B. and Gold, A.H., Soil Sci. 94, 371 (1962).

21. Jordine, E.St.A., Soil Sci., 96, 149 (1963).

22. Langmuir, I., J.Chem.Phys. 6, 873, (1938).

23. MacEwan, D.M., Nature, 162, 935 (1948).

24. Maxwell, J.C., A Treatise on Electricity and Magnetism, 3rd ed., vol. 1, Dover Publications Inc., New York.

25. Neddih, B.I., Diss.Abs., 24, 1419 (1963).

26. Norrish, K., Disc.Faraday Soc., 18, 120 (1954).

27. Norrish, K. and Russell-Colom, J.A., Clays and Clay Minerals 10, 123 (1963).

28. Russel, A., Proc.Phys.Soc., 23, 352 (1911).

29. Smith-Rose, R.L., Proc.Roy.Soc., Ser.A. 140, 359 (1933).

30. Smith-Rose, R.L., J.Inst.Elec.Engrs. 75, 221 (1934).

31. Stern, O., Z.Electrochem. 30, 508 (1924).

32. Thomson, W. (Lord Kelvin) Reprint of Papers on Electrostatics and Magnetism, MacMillan and Co., London (1872).

33. Verwey, E.J.W. and Overbeek, J.T.G., Theory of Stability of Lyophobic Colloids, Elsevier Publishing Co. Inc., New York (1948).

34. Weiss, A., Clays and Clay Minerals, 10, 191 (1963).